Distribution Agreement

In presenting this thesis as a partial fulfillment of the requirements for a degree from Emory University, I hereby grant to Emory University and its agents the non-exclusive license to archive, make accessible, and display my thesis in whole or in part in all forms of media, now or hereafter now, including display on the World Wide Web. I understand that I may select some access restrictions as part of the online submission of this thesis. I retain all ownership rights to the copyright of the thesis. I also retain the right to use in future works (such as articles or books) all or part of this thesis.

Jeffrey Bellah April 10, 2017

Investigation of Chordoma-like Tumors in Zebrafish Embryos Induced by SB-505124 Treatment

by

Jeffrey Bellah

Andreas Fritz, Ph.D.
Adviser

Department of Biology

Andreas Fritz, Ph.D.

Adviser

Iain Shepherd, Ph.D.

Committee Member

Jin-Tang Dong, Ph.D.

Committee Member

2017

Investigation of Chordoma-like Tumors in Zebrafish Embryos Induced by SB-505124 Treatment

By

Jeffrey Bellah

Andreas Fritz, Ph.D.

Adviser

An abstract of
a thesis submitted to the Faculty of Emory College of Arts and Sciences
of Emory University in partial fulfillment
of the requirements of the degree of
Bachelor of Sciences with Honors

Department of Biology

2017

Abstract

Investigation of Chordoma-like Tumors in Zebrafish Embryos Induced by SB-505124 Treatment

By Jeffrey Bellah

Chordomas are rare, malignant bone cancers that affect the axial skeleton and are believed to develop from the remnants of the notochord. Signaling by Nodal, via the TGF-beta signaling pathway, is important in the control of proliferation and differentiation in notochord development. One of the genes Nodal influences, *Brachyury*, is known to be a marker for chordomas. We have found that zebrafish embryos treated with the drug SB-505124, which inhibits the TGF-beta signaling pathway, develop tumors that resemble chordomas in their expression of *ta*, a homolog of *Brachyury*. We initially hoped to use microarray analyses of SB-505124-induced tumors and control notochord tissue to compare expression patterns of SB-505124-induced tumors with those of chordomas. In attempting to validate the microarray through *in situ* hybridizations, there were numerous inconsistencies, which suggest that the microarray results are in error, though we do not currently understand the reason why. Though the protocol for our RNAseq analysis of the tumors is still being refined before comparison with human chordoma datasets, the initial dataset has proven to be more verifiable than the microarray analyses. As an additional comparison, we have conducted *in situ* hybridizations using probes for zebrafish orthologs of published diagnostic markers for chordomas. The results suggest significant similarity to chordomas, since 4 of the 11 diagnostic markers tested so far have exhibited expression of a zebrafish ortholog in the tumors. We have identified that the signaling of the ligands *tgfb2* and *tgfb3* from the notochord to the receptor *tgfbr1b* on nearby tissues is the most likely signaling event that SB-505124 is inhibiting during tumorigenesis due to their mRNA expression patterns, which may lead to tumorigenesis in a cell non-autonomous fashion. Our inability to recreate the tumor phenotype using alternate methods of inhibiting TGF-beta signaling suggests that SB-505124 may possess a novel activity in addition to inhibiting TGF-beta signaling that plays an important role in tumorigenesis. This does not exclude a role for the inhibition of TGF-beta signaling in tumorigenesis though, because preliminary results suggest that the inhibition of TGF-beta signaling via alternative inhibitors increases tumorigenesis in low dosage SB-505124 treatments.

Investigation of Chordoma-like Tumors in Zebrafish Embryos Induced by SB-505124 Treatment

By

Jeffrey Bellah

Andreas Fritz, Ph.D.

Adviser

A thesis submitted to the Faculty of Emory College of Arts and Sciences
of Emory University in partial fulfillment
of the requirements of the degree of
Bachelor of Sciences with Honors

Department of Biology

2017

Acknowledgements

We thank the lab of Roger Deal, and particularly Marko Bajic, for assistance with RNAseq analysis and troubleshooting. We also thank Dr. Angeleen Fleming for her advice on notochord dissections and Dr. Cecilia Moens for the *shh* ArB zebrafish line. We also appreciate the services provided by the Emory Integrated Genetics Core and Georgia Genetics Facility at the University of Georgia that were used for microarray and RNAseq analyses, respectively. Thanks also goes out to Allyson Koyen and Rebecca Meador for their contributions in the lab.

Table of Contents

Introduction

Chordomas are rare tumors that develop in the vertebral column and are believed to be derived from either the nuclei pulposi or from cells trapped in the vertebrae, both of which in turn are derived from the remnants of the notochord [1, 2]. Although chordomas are rare, affecting only about one in a million people, they are highly malignant and represent approximately 3% of all bone tumors and 20% of primary spine tumors [1]. Morphologically, classical chordomas are characterized by their foamy appearance, which is due to the presence of multiple large vacuoles. Previous studies have revealed that *Brachyury*, a member of the T-box gene family of transcription factors, is expressed in >90% of chordomas, which has led to its usage as a marker for chordomas [1]. Though the majority of chordomas are sporadic in origin, a copy number gain of *Brachyury* has been associated with hereditary chordomas, suggesting that it may play a role in the formation of chordomas [2]. In vertebrates, *Brachyury* is expressed in the developing notochord, a mesodermal structure under the neural tube that signals the differentiation of nearby tissues. In the mature notochord though, *Brachyury* is no longer expressed, so *Brachyury* expression in chordomas supports the theory that chordomas are derived from notochord cells that have reverted to a more "embryonic" state [1]. *Brachyury* expression in the notochord is regulated by multiple essential signaling pathways, including signaling by ligands of the transforming growth factor beta (TGF-β) superfamily [1]. Another important marker of chordomas is the gene *sonic hedgehog* (*shh*), which, like *Brachyury*, is expressed in the developing notochord but not in mature notochord cells [3]. The expression of these genes in chordomas therefore supports the idea that they are derived from notochord cells that return to an embryonic, proliferative state.

In addition to *Brachyury*, signaling through *mechanistic target of rapamycin* (*mTOR*) has been implicated in chordomas [4]. mTOR signaling has been found in about 65% of chordomas based off of the levels of phosphorylated mTOR and phosphorylated ribosomal protein S6 kinase beta-1 (p70S6K), an effector of mTOR signaling [4]. Furthermore, crosstalk has been reported between TGF-β signaling and elements of mTOR signaling, which suggests a possible link between *Brachyury* expression and mTOR activation in chordomas [5]. Though the exact mechanism is uncertain, a TGF-β receptor complex bound to a TGF-β ligand can activate phosphoinositide 3-kinase (PI3K) [6]. In turn, PI3K, through established intermediates, activates mTOR [7]. Active mTOR activates p70S6K, which phosphorylates ribosomal protein S6 as a primary effector of the inhibition of growth arrest. An opposing force on the phosphorylation of ribosomal protein S6 can also come from TGF-β signaling. Activated TGF-β type I receptors recruit the Bα subunit of protein phosphatase 2 (PP2A), which increases PP2A's inhibition of p70S6K, therefore decreasing the phosphorylation of ribosomal protein S6 [5]. Due to the ability of TGF-β signaling to modulate both *Brachyury* expression and mTOR activity, it may play a role in chordoma formation, which has been supported by the finding of copy number variations in TGF-β ligands and receptors in some chordomas [8].

The TGF-β signaling pathway is important in notochord development, which further links it to chordomas. The role of TGF-β superfamily ligands, specifically Nodal and the bone morphogenic proteins (BMPs), on notochord development has been studied in zebrafish embryos. Nodal and BMP signals are required at mid-blastula transition to specify tail tissues, whereas Nodal signals without BMP signals specify tissues that will form the axis, including the chordamesoderm cell fate that will become the notochord [9]. Important readouts of actively proliferating notochord are the zebrafish homologs of *Brachyury*, *T, Brachyury homolog a* (*ta*)

and *T, Brachyury homolog b* (*tb*), and the zebrafish homologs of *shh*, *sonic hedgehog a* (*shha*) and *sonic hedgehog b* (*shhb*). One tool that has been used to study the role of Nodal signaling in notochord development in zebrafish has been the small molecule drug SB-505124, which inhibits Nodal signaling but not BMP signaling. This is possible because Nodal ligands and BMP ligands use different receptors.

Receptors for TGF-β superfamily ligands are heteromeric complexes composed of two TGF-β type I receptors and two TGF-β type II receptors [5]. TGF-β type I receptors are activin receptor-like kinases (ALKs). Whereas the TGF-β receptor complex for BMP ligands uses either ALK2, ALK3, or ALK6 as the TGF-β type I receptors, the TGF-β receptor complex for Nodal, TGF-β, and Activin ligands uses either ALK4, ALK5, or ALK7 as the TGF-β type I receptor. When the ligand forms a complex with the type I and type II receptors, the serine/threonine kinase domain of the type II receptors phosphorylate the type I receptors to activate the type I receptors [10]. In the canonical SMAD-mediated pathway, the type I receptors then phosphorylate R-SMAD proteins via their own serine/threonine kinase domain [5]. The phosphorylated R-SMADs complex with SMAD4, the co-SMAD, before translocating to the nucleus where they regulate gene transcription and may promote cellular processes such as apoptosis, epithelial to mesenchymal transition, or growth arrest [5].

Zebrafish have been used as tumor models through a variety of methods including chemical mutagenesis, mutant lines, transgenic lines, and xenotransplantation of cancer cells [11]. In recent years, zebrafish tumor models have begun to be used for small molecule therapeutic drug screening as a method of rapid *in vivo* drug screening for cancer therapies [12]. Two zebrafish models of chordoma have been reported in recent years. The first zebrafish model of chordoma was reported in a transgenic line that used the *shhb* promoter region to drive

expression of a constitutively active form of the human gene: *HRas proto-oncogene, GTPase* (HRASV12) [13]. They assert its similarity to chordomas primarily due to the presence of Brachyury and Cytokeratin, an immunohistochemical marker of chordoma, and similarities in cell pathology using hematoxylin and eosin (H&E) staining. The most recent zebrafish model of chordoma reported that the overexpression of phosphatase of regenerating liver-3 (PRL-3) by injecting one-cell stage embryos with the mRNA of zebrafish or human PRL-3 caused the notochord to develop a phenotype resembling chordoma [14]. This model is connected to chordomas by its expression of *ta* and *shha* and similarities in cell pathology using H&E staining.

We report that treatment of zebrafish embryos around the 18-somite stage with SB-505124 causes the embryos to develop chordoma-like tumors from the notochord. SB-505124 has been shown to inhibit signaling by ALK4, ALK5, and ALK7 (most potently ALK5) by competitively binding to the ATP-binding site of the kinase domain, therefore likely inhibiting signaling through Activin, Nodal, and TGF-β ligands [15]. Treatment with SB-505124 during mid-blastula transition mimics loss of Nodal signaling and caused zebrafish embryos to develop cyclopia, mirroring the phenotype of a double knockout line of the two zebrafish Nodal ligands [16]. These SB-505124-induced tumors resemble chordomas in that they express *ta* and *tb*, the zebrafish homologs of *Brachyury*, and over a third of the diagnostic markers for chordomas, including *ta*. They also express additional markers of proliferative notochord including *shha* and *shhb*. We have identified that the signaling of the ligands *tgfb2* and *tgfb3* from the notochord to the ALK5 receptor *tgfbr1b* on nearby tissues is the most likely signaling event that SB-505124 is inhibiting during tumorigenesis due to their mRNA expression patterns, which may lead to tumorigenesis in a cell non-autonomous fashion. In addition, our results suggest that SB-505124

may possess a novel activity in addition to the inhibition of ALK4, ALK5, and ALK7 that plays an important role in tumorigenesis. This does not exclude a role for the inhibition of ALK4, ALK5, and ALK7 in tumorigenesis though, because preliminary results suggest that the inhibition of ALK4, ALK5, and ALK7 via means other than SB-505124 increases the amount of tumorigenesis that occurs during low dosage SB-505124 treatments. We have also developed transgenic lines expressing fluorescent protein in the SB-505124-induced tumors that may be used for quantitative measures of tumor formation and size during high-throughput drug screens. We have shown that the SB-505124-induced tumorigenesis is inhibited by rapamycin, which therefore may be used as a positive control during drug screens. Rapamycin's inhibition of tumorigenesis also suggests that activation of the mTOR pathway is important for tumorigenesis, though how SB-505124 treatment leads to mTOR pathway activation is currently unknown.

Materials and Methods

Drug Treatment

Embryos were collected on day 1 and left to develop overnight at room temperature with a density of approximately 150 per petri dish. On day 2, embryos were dechorionated. When the embryos reached 16-20 somites on day 2, their media was replaced with embryo media containing the drug. Unless specified otherwise, SB-505124 was used at either 40μM or 50μM. Embryos were then left to develop for 48 hours at 28°C, with any dead cleaned off on day 3. After 48 hours of drug treatment, the drug media was removed and replaced with embryo media.

Histopathology

SB-505124 or DMSO (vehicle control) treated embryos were fixed in 4% paraformaldehyde in 1x PBS at 5 days post-fertilization (dpf). Fixed embryos were embedded into paraffin, sectioned

using a microtome (5 and 10μM thick), and stained with hematoxylin and eosin by the Emory Pathology Core at Yerkes National Primate Research Center.

Dissection of Notochord and Tumors

Embryos for dissection were anesthetized using tricaine prior to dissection. Once embryo movement and touch response ceased, embryos were placed in 1x PBS with SYLGARD® 184 coating the bottom of the dish. Minutien needles were used to pin the embryo to the dish, being careful not to damage the notochord. A MICRO FEATHER® ophthalmic micro scalpel was used to first decapitate the embryo. For notochord dissections, the tail was also cut off at the end of the notochord, because the notochord seems to be anchored more tightly at the posterior tip. Fine forceps were used to grab the anterior end of the notochord while a fine needle was used to carefully separate nearby tissues from the notochord. For tumor dissections, the tools were used to cut the epidermis surrounding the tumor and extract the tumor through the opening created. A siliconized 200μL pipette tip was used to transfer the isolated notochords or tumors to Qiazol/Trizol for immediate total RNA isolation or to RNAlater for storage until total RNA isolation.

Microarray Analyses

Microarray analyses were conducted on notochord or tumor dissections by the Emory Integrated Genomics Core using Affymetrix GeneChip Zebrafish Genome Array chips. The data and statistical analyses provided by Emory Integrated Genomics Core on our microarray analyses were used to identify significantly up regulated and down regulated genes. The ZFIN Database was used to find expression data for these genes when available.

RNAseq Analysis

Initial RNAseq analysis was done by sending the isolated total RNA from our dissections to the Deal Lab, who prepared it for RNAseq analysis. RNAseq analysis was then conducted by the Georgia Genomics Facility at the University of Georgia. The raw dataset was processed and aligned to the zebrafish transcriptome with aid from the Deal Lab. Troubleshooting the cause of short fragments was done with assistance from the Deal Lab using whole embryo total RNA isolated from zebrafish embryos. The concentration following polyA selection was checked to make sure that we didn't lose an abnormally large amount of RNA during polyA selection. The fragmentation protocol was tested by halving the fragmentation time of the typical Deal Lab protocol and comparing it to the normal fragmentation time by running the amplified fragments on an agarose gel.

Primer Synthesis

Primers for *in situ* probes were generated using EditSeq and PrimerSelect from the DNASTAR Lasergene Suite based on cDNA sequences obtained from the National Center for Biotechnology Information for chosen genes, and subsequently purchased from Integrated DNA Technologies.

RNA *in situ* Probe Synthesis

Primers designed to amplify a 700-1100 bp fragment of the target gene were used to amplify the chosen fragment via RT-PCR (QIAGEN OneStep RT-PCR), which was cloned into a pCR®II-TOPO® vector using Invitrogen™ One Shot® Top10 Chemically Competent *E. coli*. The plasmid was then linearized and the probe was synthesized using T7 or SP6 RNA polymerase.

RNA *in situ* Hybridization

Whole-mount RNA *in situ* hybridizations were performed using all synthesized probes on SB-505124 treated and DMSO treated (vehicle control) embryos following the protocol by Thisse and Thisse on the ZFIN Database (https://zfin.org/ZFIN/Methods/ThisseProtocol.html).

Transgenic Line Generation

The regulatory region of *shha* (activator region C [ArC], identified by Müller et al.) or *ta* (identified by Harvey et al.) was amplified via PCR and cloned into the pDEST R4-R3 Vector II destination vector using the MultiSite Gateway® Three-Fragment Vector Construction Kit, along with GAL4 and minimal promoter sequences in order to create *shha*-GAL4 and *ta*-GAL4 constructs [17, 18]. The constructs were co-injected with Tol2 mRNA directly into the cell of 1-cell stage UAS-Kaede zebrafish embryos in order to generate *shha*-GAL4:UAS-Kaede and *ta*-GAL4:UAS-Kaede fish.

Results

Preliminary Characterization of SB-505124-Induced Tumors

We found that treating zebrafish embryos from the 10-somite stage through the 22-somite stage with 40μM SB-505124 resulted in the formation of tumors that appeared to be connected to the notochord within 48 hours of the treatment beginning (**Figure 1**). Embryos treated at later stages generally had more easily distinguished tumors, because the earliest treated embryos also developed severe kinking of the notochord that was often hard to distinguish from tumors. The tumors are not limited to the actively proliferating end of the notochord, but also appear in the more matured anterior sections of the notochord. By 5 days post-fertilization, the tumor phenotype exhibited near 100% penetrance. Treatments with lower concentrations of SB-505124 resulted in a lower number of tumors per embryo and a decreased penetrance (**Figure 2**).

With the aim of probing the cellular origin of the tumors, initial RNA *in situ* hybridizations for markers of proliferative notochord revealed that the zebrafish homologs of *Brachyury*, *ta* and *tb*, the zebrafish homologs of *shh*, *shha* and *shhb*, and *collagen, type II, alpha*

1a (*col2a1a*) are all expressed in the tumors (**Figure 3A-E**). Furthermore, antibody staining against phosphorylated ribosomal protein S6 (pS6), a downstream effector of mTOR signaling that is correlated with increased inhibition of growth arrest, found that pS6 is present at significantly higher levels in the tumors compared to nearby tissues and notochord (**Figure 3F**). Since the previous two chordoma models identified in zebrafish observed the histopathology of their tumors for similarities to chordomas, we stained sections of SB-505124-induced tumors and DMSO treated control notochords with H&E. Initial results from the H&E staining show that the cells making up the tumor mass appear similar to the vacuolated cells of the notochord in a disorganized state and are also reminiscent of the vacuolated cells found in chordomas (**Figure 4**). These results suggest that the SB-505124-induced tumors are notochord-derived in that they express proliferative notochord markers and appear similar in H&E staining. In addition, they indicate an initial similarity to chordomas in that *Brachyury* is expressed and mTOR is overactivated.

Comparison of SB-505124-Induced Tumors and Chordomas

To identify the degree of similarity between the SB-505124-induced tumors and chordomas, it will be beneficial to compare transcriptomic data from the SB-505124-induced tumors with published transcriptomic data from chordomas, which requires the separation of tumor cells from other surrounding cell types (http://xavierlab2.mgh.harvard.edu/chordoma/index.html). Toward this end, we developed dissection techniques to isolate the tumors and control notochords. The initial dissection technique involved cutting out portions of the trunk containing the tumor from SB-505124 treated embryos or portions of the trunk containing notochord from dimethyl sulfoxide (DMSO, vehicle) treated control embryos. These initial dissections were used to compare tumor and

notochord expression in a microarray analysis. Since most of the genes were not involved in the notochord or tumors, we concluded that the presence of trunk tissue skewed the data too severely to use it to identify significantly altered gene ontology terms for comparison with chordoma datasets. To improve upon this approach, we got advice on notochord dissections from Angeleen Fleming, Ph.D., who had previously isolated zebrafish notochords for culture [19]. Using her advice and transgenic lines with fluorescently labeled notochord and tumor cells for easier visualization, we refined our dissection techniques to isolate just the tumors or notochord (**Figure 5**).

Using the refined dissection technique, we isolated SB-505124-induced tumors and wild-type notochord from embryos of the same age, which we then compared using a microarray analysis. The microarray analysis data was sorted based off the fold-change in expression and the statistical significance using the p-value. We identified strongly upregulated or downregulated genes for which we created RNA *in situ* hybridization probes in order to visualize their expression in wild-type and SB-505124 treated embryos as a method to verify the accuracy of the microarray analysis, and we noted which of those genes had known notochord expression on the ZFIN database. We successfully made probes for 50 genes identified from the microarray analysis, but only 3 of the genes exhibited the expression patterns predicted by the microarray analysis: *notochord granular surface* (*ngs*), *EH-domain containing 2b* (*ehd2b*), and *complement component 7a* (*c7a*), all of which were upregulated in tumors (**Figure 6**). Furthermore, the RNA *in situ* hybridizations of *ta*, *tb*, *shha*, and *shhb* would suggest that they should be identified as significantly upregulated in the microarray analysis, but none of them were identified in the microarray analysis (**Figures 1A-D and 7**). In addition, many of the genes with expression data on ZFIN were not expressed in the notochord. Because we were unable to verify the accuracy of

the microarray analysis, we were unable to compare it with transcriptomic chordoma data, though the reasons for the inaccuracy of the microarray are unclear. Despite the inaccuracy of the microarray analysis, the verification attempts did yield 3 new markers of SB-505124-induced tumors that may be used to verify future transcriptomic data and that further characterize gene expression changes in the SB-505124-induced tumors.

Since RNAseq data for chordomas has been released, we have initiated RNAseq analysis with our dissected-out tumors and wild-type notochords to compare the full transcriptomes. The results of a test RNAseq analysis using one tumor sample indicated that the distribution of read lengths was abnormally biased toward shorter reads and of low quality. To correct this, we have been working with the Deal Lab to identify the step in the RNAseq analysis preparation that led to this by altering single steps of the procedure to see how it effects our number or length of reads. We found that the fragmentation protocol that they initially used likely over-fragmented the mRNA, resulting in the shorter reads, and that using a shorter fragmentation time will yield more normal length fragments for sequencing (data not shown). Though RNAseq analysis results using the updated fragmentation protocol have not yet been obtained, we used the test RNAseq analysis results to pick 3 genes with high read counts in the SB-505124-induced tumors that are normally expressed in the notochord and created RNA *in situ* hybridization probes for them. Though we are still working on creating the probe for one of the genes, *glypican 5a* (*gpc5a*), we successfully created probes for the other 2 genes, *polymerase I and transcript release factor b* (*ptrfb*) and *synuclein, gamma a* (*sncga*), which both showed expression in the SB-505124-induced tumors (**Figure 8**).

As an additional method of comparing important gene expression in the SB-505124-induced tumors and chordomas, we created RNA *in situ* hybridization probes for the zebrafish

homologs of the genes that have been identified as diagnostic markers for chordomas in the literature based off chordoma transcriptomic data (http://xavierlab2.mgh.harvard.edu/chordoma/index.html). Though one of the diagnostic marker genes did not have an easily identifiable zebrafish homolog, we created probes for the other 11 published markers and found that 4 of these diagnostic markers are expressed in the SB-505124-induced tumors (**Figure 9**). Therefore, over a third of the diagnostic markers are expressed in SB-505124-induced tumors. Though there is the possibility that some of the probes we made may have been of poor quality and thus yielded false negative results, most of the probes showed at least some amount of specific expression in wild-types, suggesting that our probes would accurately report the genes' expression patterns in SB-505124 treated embryos (data not shown). Furthermore, when we investigated the test RNAseq analysis data for the presence of the diagnostic marker genes, we found that the RNAseq analysis data included 10 of the 12 genes and out of these 10, 6 of the genes had a significant number of transcripts (*acanb*, *col2a1a*, *cspg4*, *enpp1*, *ta*, and *wwp2*), including all 4 diagnostic marker genes that we had already identified as being expressed in the SB-505124-induced tumors. These results suggest that the SB-505124-induced tumors likely possess sufficient similarity to chordomas to serve as a model, though further experiments are needed to refine our understanding of the similarities.

How Does SB-505124 Induce Tumorigenesis?

The most straightforward mechanism for SB-505124-induced tumorigenesis would be a cell autonomous function of SB-505124, in which it inhibits a signaling event in notochord cells. To address this hypothesis, we wanted to see which signaling events that SB-505124 is known to inhibit may be occurring in the notochord during SB-505124 treatment. To do this, we first identified established and potential zebrafish orthologs of human and mice ALK4, ALK5, and

ALK7 using BLASTp and BLASTx (https://blast.ncbi.nlm.nih.gov/Blast.cgi). We identified 6 different potential orthologs, of which 5 were previously identified (shown in **Table 1**). We used RNA *in situ* hybridizations for the mRNA of the ALK4, ALK5, and ALK7 zebrafish orthologs to identify which tissues are expressing these receptors during or prior to SB-505124 treatment. Most of the receptors were expressed in the notochord during bud and 2-somite stages, but by the 8 to 10-somite stages, none were expressed in the notochord (**Table 1** and **Appendix**). Despite the lack of notochord expression, at the 8-somite stage, *transforming growth factor, beta receptor 1 a* (*tgfbr1a*, an ALK5), *activin A receptor, type IBa* (*acvr1ba*, an ALK4), and *activin A receptor, type IBb* (*acvr1bb*, an ALK4) did show expression in an undetermined axial structure that was ventral of the notochord, though even that expression was gone by around the 10 to 12-somite stages. An additional gene, *transforming growth factor, beta receptor 1 b* (*tgfbr1b*, an ALK5), also had expression in the axial structure ventral of the notochord at the 10-somite stage, which persisted through the 16-somite stage, in addition to expression in the somites at the same time (**Figure A2**).

As the TGF-β superfamily ligands that utilize ALK4, ALK5, or ALK7 (Nodal, TGF-β, and Activin) are better characterized than the receptors, we first screened their published expression on the ZFIN Database. The ZFIN Database search revealed that both of the zebrafish Nodal ligands and the zebrafish TGF-β ligands *transforming growth factor, beta 1a* (*tgfb1a*) and *transforming growth factor, beta 1b* (*tgfb1b*) are not expressed in or adjacent to the notochord prior to or during SB-505124 treatment, so we did not create probes for these genes. The ZFIN Database search also showed that the zebrafish TGF-β ligands *transforming growth factor, beta 2* (*tgfb2*) and *transforming growth factor, beta 3* (*tgfb3*) are likely expressed in the notochord at developmental timepoints relevant to the SB-505124 treatments, so we made probes for *tgfb2*

and *tgfb3*, in addition to probes for the activin subunits *inhibin, beta B* (*inhbb*) and *inhibin, beta Ab* (*inhbab*), for which the expression patterns are unknown. RNA *in situ* hybridization assays using these probes confirmed that *tgfb2* and *tgfb3* are both expressed in the notochord prior to and during the beginning of the SB-505124 treatment (**Figure 10A-B**). Neither *inhbb* nor *inhbab* were expressed in or near the notochord at the appropriate time points to be relevant to SB-505124 treatment (**Figure 10C-D**).

Since *tgfb2* and *tgfb3* are the most likely ligands whose signaling is being inhibited by SB-505124 treatment, we investigated the effect of antisense-mediated morpholino knockdown of *tgfb2* and *tgfb3*. We used both splice-blocking and translation-blocking morpholinos to knockdown *tgfb2* and *tgfb3*. Singular knockdowns or the combined knockdown of both *tgfb2* and *tgfb3* did not develop the tumor phenotype, though the notochord cells of the knockouts did appear more rounded and bunched on top of each other, rather than forming the row of cuboidal cells that make up the notochord in uninjected embryos (**Figure 11**).

These results suggest that SB-505124-induced tumorigenesis may be caused by the inhibition of *tgfb2* and/or *tgfb3* signaling in a cell non-autonomous fashion or by an additional, uncharacterized activity.

Alternative Inhibitors of ALK4, ALK5, and ALK7

Though the temporal difference between the morpholino knockdown of *tgfb2* and *tgfb3* and SB-505124 treatment may be the reason that the morpholino knockdown failed to develop the tumor phenotype, another possibility is that SB-505124 may possess additional, uncharacterized activity in addition to its inhibition of ALK4, ALK5, and ALK7, and this additional activity is necessary for tumorigenesis. To begin probing this question, we acquired additional small molecule inhibitors of ALK4, ALK5, and ALK7 that have various chemical

structures: SB-431542, SD-208, A83-01, and GW788388. The maximum concentration tested was determined either by the severity of the phenotype of the treated embryos or by the formation of precipitate during treatment (SB-431542 and GW788388 due to precipitate; SD-208 and A83-01 due to phenotypic severity). All four additional inhibitors failed to recapitulate the tumor phenotype (**Figure 12**). As a control for the more efficient inhibitors (SD-208 and A83-01), we treated 2.75 hours post fertilization embryos with SB-505124, SD-208, or A83-01 as per Hagos and Dougan's (2007) procedure for using SB-505124 to recapitulate the nodal morphant phenotype. Though the severity each drug caused varied, all 3 treatments recapitulated the cyclopia phenotype of nodal morphants (data not shown).

Since SD-208 and A83-01 were confirmed as having similar nodal inhibiting activities to SB-505124, but differing structures (and thus possibly different off-target effects), we used them for initial experiments probing the requirement of SB-505124's inhibition of ALK4, ALK5, and ALK7 for tumorigenesis. To do this, we used a low penetrance concentration of SB-505124 and either treated the embryos with only SB-505124, both SB-505124 and A83-01, or SB-505124 and SD-208. The number of tumors per embryos and overall penetrance would then be calculated for each treatment at 5 days post fertilization. Though only preliminary results have been obtained and the concentrations of A83-01 and SD-208 still need to be refined, the preliminary results suggest that SD-208 increased the number of tumors per embryo and the penetrance of the tumor phenotype (**Figure 13**).

The inability of the alternative inhibitors to recreate the tumor phenotype suggests that SB-505124 may possess an additional activity that the other inhibitors lack, which is necessary for tumorigenesis to occur. Because SD-208 treatment increases the tumor phenotype of SB-

505124, it is likely that the inhibition of ALK4, ALK5, and ALK7 does play a role in tumorigenesis, though it appears not to be sufficient to induce tumorigenesis alone.

Testing the Feasibility of Using SB-505124-Induced Tumors for Drug Discovery

Recent studies have shown that zebrafish are ideal for small chemical screens [12]. For a drug discovery screen, it would be optimal to have a tumor marker in live embryos to observe the effect of the drugs on the tumors. Toward this end, we wanted to create a transgenic zebrafish line that will express the fluorescent protein Kaede in the tumors. Harvey et al. had previously created a transgenic line using *ta* regulatory elements to drive expression of a fluorescent protein in the notochord, which we attempted to recreate, but the fluorescence of the line was poor (data not shown) [17]. Since *shha* is also a strong marker of the proliferative notochord and SB-505124-induced tumors and has relatively well characterized regulatory sequences, we decided to use it to drive Kaede expression [18]. Though there are multiple regulatory sequences for *shha*, the activator region C (ArC) is the only one that has been characterized as being specific to the notochord, so we used ArC to drive Kaede expression in the *shha* driven Kaede transgenic line [18]. We also acquired a *shha* driven GFP transgenic line from Cecilia Moens, though this was under control of the *shha* activator region B (ArB), which drives floorplate expression of *shha* [C. Moens, personal communication]. Interestingly, a small group of the ArB fish expressed GFP in the notochord instead of the floorplate, which we isolated to form the *shha* ArB* line (**Figure 14A-B**). In addition, the *shha* ArC line we generated had strong Kaede expression in the developing notochord and in SB-505124-induced tumors (**Figure 14C**). Though the transgenic *shha* ArC and ArB* lines have been established, a technique for using fluorescence as a measure of tumor size has not yet been developed.

For drug screens, controls are necessary, so the development of a positive drug treatment control that decreases SB-505124-induced tumorigenesis would be useful for high-throughput drug screens utilizing SB-505124 treated embryos. Rapamycin and its analogs, which inhibit mTOR activity, have been shown to affect chordoma cell growth in culture and slow down the growth of the HRASV12 driven zebrafish chordoma model [13, 20]. Since we have also found that pS6 is present in significant quantities in SB-505124-induced tumors, which is suggestive of mTOR pathway activity, the use of rapamycin was hypothesized as a drug treatment that would decrease tumor counts and penetrance (**Figure 3E**). Treatment of embryos with both SB-505124 and rapamycin or SB-505124 followed by rapamycin significantly decreased the number of tumors per embryo (**Figures 15 and 16**). Furthermore, the tumors present in embryos treated with rapamycin appeared to typically be smaller than normal SB-505124-induced tumors, though this was not quantitatively measured.

Discussion

SB-505124-Induced Tumors as a Model for Chordoma

Here we show that treatment of 10 to 22-somite zebrafish embryos with SB-505124 induces the efficient formation of tumors of notochord origin that appear to model chordoma. The apparent connection of the SB-505124-induced tumors to the notochord and the expression of the proliferative notochord markers *ta*, *tb*, *shha*, and *shhb* in SB-505124-induced tumors supports our observations that they are derived from notochord cells. Due to the notochordal origin of the SB-505124-induced tumors and their expression of both zebrafish homologs of *Brachyury*, an important marker of chordoma, we hypothesized that the SB-505124-induced tumors might share sufficient similarities with chordomas to serve as a chordoma model for

screens of potential drug therapies. This hypothesis was further supported when we assayed the tumors for expression of the 12 diagnostic marker genes for chordomas. Though just over a third of the genes for which there was a zebrafish homolog were expressed in the SB-505124-induced tumors, which may seem insignificant, the markers genes are for diagnostic purposes and therefore do not represent a suite of genes that are expressed in all chordomas. Rather, any chordoma is expected to express some subset of the diagnostic genes, which our SB-505124-induced tumors did, so this supports the tumors as a model for chordoma.

Ultimately, a complete transcriptome comparison, focusing both on genes with high absolute read counts and on genes with significant changes in regulation compared to normal notochord, of the SB-505124-induced tumors with chordomas will be the best measure of how close of a model the SB-505124-induced tumors will be for chordomas. Our initial attempts to do this by using dissected-out tumors and wild-type notochords in microarray analyses failed to yield verifiable results since only 3 of the 50 genes we made probes for showed the predicted expression and *ta*, *tb*, *shha*, and *shhb* were not identified by the microarray analyses as being significantly upregulated in the tumors, though the reason for the inaccuracy of the microarray analyses remains unclear.

A more successful attempt at transcriptome comparison has been begun by using RNAseq analysis on dissected-out SB-505124-induced tumors. We are still optimizing the fragmentation protocol of the RNAseq analysis to have a normal distribution of read lengths, and therefore do not have a final transcriptome to compare with transcriptomic data from chordomas. Despite this, the initial test RNAseq analysis that we did suggests that the RNAseq analyses are more accurate than the earlier microarrays analyses, since the first two notochord genes with high read counts in the tumors that we made RNA *in situ* hybridization probes both showed the

expected strong expression in SB-505124-induced tumors. This is further supported by *ngs*, one of the novel SB-505124-induced tumor markers identified from the microarray analyses, having one of the highest read counts in the test RNAseq analysis (data not shown).

Between the new markers for the SB-505124-induced tumors that were identified from the microarray analyses, the initial test RNAseq analysis, and diagnostic markers list, we have obtained a preliminary understanding of the transcriptome of the SB-505124-induced tumors, which will be significantly improved when the final RNAseq analysis dataset is obtained. Despite the current incomplete nature, several of the genes we've identified, such as *col2a1a*, *cspg4*, and *acanb*, are involved in extracellular matrix formation, an important step in chondrogenesis (the development of cartilage). It has been noted that one of the main pathways activated in chordomas is chondrogenesis, so the expression of these genes in the SB-505124-induced tumors suggests that similar chondrogenesis events may play an important role in both SB-505124-induced tumors and chordomas (http://xavierlab2.mgh.harvard.edu/chordoma/index.html). Furthermore, though the initial RNAseq analysis is not optimal, early verification attempts have been positive and half of the diagnostic marker genes (6/12) for chordomas are being expressed in the tumors per the initial RNAseq analysis, which suggests further similarity beyond the 4 diagnostic genes identified by RNA *in situ* hybridization assays. Due to the similarities between SB-505124-induced tumors and chordomas, understanding how the SB-505124-induced tumors form may lead to identification of risk factors for sporadic chordomas.

Mechanism of SB-505124-induced Tumorigenesis in Zebrafish Embryos

When investigating the mechanism by which SB-505124-induced tumors form, we started with the simplest hypothesis: SB-505124 induces tumorigenesis through a cell

autonomous effect on notochord cells. To test this, we wanted find what signaling events that SB-505124 is known to inhibit occur in the notochord during SB-505124 treatment. To identify which ligand-receptor combinations were present in or near notochord tissue during SB-505124 treatment, we did RNA *in situ* hybridizations for predicted zebrafish homologs of ALK4, ALK5, and ALK7 TGF-β type I receptors and their ligands for which expression data at the correct developmental stages was not available. Though in humans there is ALK4, ALK5, and ALK7, we identified 6 possible receptors, which is explained because zebrafish have undergone a genome duplication in their ancestry since diverging with humans [21]. With regards to the ligands, we found that *tgfb2* and *tgfb3* are expressed in notochord cells throughout the beginning of SB-505124 treatment, which suggests that SB-505124 is inhibiting their signaling. Though many of the receptors that we identified were expressed in or around the notochord at early somitogenesis, most of them were turned off well before the time of SB-505124 treatment. There is a slight possibility that *tgfbr1a*, *acvr1ba*, and *acvr1bb* may be present in the unidentified ventral axial structure during treatment though, depending on how long enough of the receptor persists in the cellular membranes to functionally signal after mRNA transcription has ceased. The most likely receptor though is *tgfbr1b*, which, even though it isn't in the notochord during treatment, is expressed in the somites and the unidentified ventral axial structure up through the beginning of SB-505124 treatment. This leaves four main possibilities. The first possibility: a subset of the receptors have a sufficiently long half-life to functionally persists in notochord cells long enough to have their signaling inhibited significantly by SB-505124 treatment. The second possibility: SB-505124 may act in a cell autonomous fashion on the notochord if there is an additional zebrafish homolog of ALK4, ALK5, or ALK7 that we did not identify and is present in the notochord during SB-505124 treatment. The third possibility: SB-505124 may act in a cell

non-autonomous fashion on the notochord by inhibiting signaling through *tgfbr1b* in the somites and unidentified ventral axial structure, which leads to these structures signaling notochord cells to become tumorigenic. The fourth possibility: SB-505124 may have additional activity in addition to the inhibition of ALK4, ALK5, and ALK7, and this additional activity plays a key role in inducing tumorigenesis.

Except for the fourth mechanism that supposes a novel activity of SB-505124, the other three mechanisms all hypothesize that tumorigenesis is due to the inhibition of *tgfb2* and/or *tgfb3* signaling, merely differing in where and what the relevant receptors are. To further investigate the role of *tgfb2* and *tgfb3* signaling in tumorigenesis, we used morpholinos to knockdown these ligands. Though the morphant embryos did not develop the tumor phenotype, this does not necessitate that SB-505124 induces tumorigenesis via a novel, unreported activity. Morpholinos are injected into the yolk of the embryo prior to the 8-cell stage so that morpholinos are present in each cell. Though morpholinos are biologically stable, so their degradation is not a major concern, unequal distribution and/or dilution during development may result in a decreased and variable efficiency of knockdown of signaling relative to SB-505124 treatment by around the 18-somite stage when SB-505124 treatment typically began. Furthermore, the knockdown of *tgfb2* and *tgfb3* signaling by the morpholinos prior to the developmental stages that SB-505124 can be added to induce tumorigenesis may introduce altered transcriptional states in notochord cells already that act against tumorigenesis. Despite the lack of tumor formation in the morphant embryos, the phenotype of notochord cells in the morphants does resemble the phenotype of non-tumor notochord cells in SB-505124 treated embryos, which suggests that at least part of the SB-505124 treated embryos' phenotype is due to the inhibition of *tgfb2* and *tgfb3* signaling.

To investigate the possible role of any additional, novel activity of SB-505124 on tumorigenesis, we used alternative small molecule drugs that have been characterized to inhibit ALK4, ALK5, and ALK7 and have chemical structures with various degrees of similarity to SB-505124. Two of these drugs, SB-431542 and GW788388, created minimal phenotypes at their maximum doses when precipitate formed in the media during treatment. This suggests that these two drugs had some bioavailability issues that prevented the active drug from reaching tissues, including the notochord, that use ALK4, ALK5, or ALK7 for signaling during the duration of the treatment. This result for SB-431542 made sense, since an earlier paper that used SB-431542 and SB-505124 to inhibit Nodal signaling at mid-blastula transition required only 50μM SB-505124 to achieve the phenotype, whereas the same phenotype could only be achieved with 800μM SB-431542 on embryos that were also physically damaged to increase the drug's availability [16]. The other two inhibitors though, SD-208 and A83-01, developed severe phenotypes similar to the SB-505124 phenotype at relatively low concentrations compared to SB-505124, though SD-208 or A83-01 treated embryos did not develop the tumor phenotype. Since both SD-208 and A83-01 also recreated the cyclopia phenotype of SB-505124 reported by Hagos and Dougan as a result of inhibiting nodal signaling after the mid-blastula transition, it seems that their inhibition of TGF-β signaling is extremely similar to that of SB-505124, which suggests that SB-505124-induced tumorigenesis may hinge up some differential activity of SB-505124 [16]. Whether this difference is due to SB-505124 having a novel tumorigenic activity or differences in the drugs' effects on a crosstalk event that is critical to tumorigenesis is unclear. Since cotreating embryos with low concentrations of SB-505124 and SD-208 increases tumor incidence compared to just the low concentration of SB-505124 by itself, it is likely that the inhibition of TGF-β signaling

does still play a role in SB-505124-induced tumorigenesis, though it may not be the only driving force.

One driving force behind SB-505124-induced tumorigenesis appears to be mTOR signaling because cotreatment with rapamycin, which inhibits mTOR activity, significantly decreases the tumor incidence compared to treatment with the same concentration of SB-505124 by itself. This suggests that the inhibition of growth arrest by pS6, which is increased by mTOR signaling, plays an important role in driving tumorigenesis, but the intermediate steps connecting SB-505124 treatment to an increase in pS6 are uncertain. One possibility would be that SB-505124 inhibits only the ability of the TGF-β type I receptor to phosphorylate the R-SMAD, in which case SB-505124 will have blocked the SMAD-mediated growth arrest signal, shifting the balance toward more proliferative signals. Alternatively, SB-505124 may inhibit both the SMAD-mediated pathway and crosstalk with the mTOR signaling pathway. In that case, since TGF-β signaling is generally associated with an overall increase in growth arrest, then removal of the entire TGF-β signal would also shift the balance of inputs to mTOR signaling such that other signals activating mTOR may become more dominant and lead to the increase in pS6 and inhibition of growth arrest.

Drawing these results together, it is still unclear what combination of the four proposed mechanisms leads to SB-505124-induced tumorigenesis. The inability of the alternate inhibitors to recreate the tumor phenotype suggests that SB-505124 utilizes some additional, novel activity during tumorigenesis, but the increased tumorigenesis in the cotreatment with SD-208 suggests that the inhibition of ALK4, ALK5, and ALK7 might play a necessary, if not sufficient, role in tumorigenesis. The mRNA expression patterns of the receptors suggest that the affected TGF-β type I receptor is most likely *tgfbr1b*, acting on the notochord in a cell non-autonomous manner,

but the lack of data on the presence of the receptor proteins themselves leaves open the possibility of long-lived receptors in the notochord acting in a cell autonomous manner too. Though RNA *in situ* hybridizations indicate where a gene is being transcribed, they are an inferior method to antibody stains or Western Blots for assaying whether the protein product is present in a tissue. Due to the lack of available antibodies against the ALK4, ALK5, and ALK7 variants we investigated, RNA *in situ* hybridizations were used as an expedient estimation of where the TGF-β type I receptors were during development. Because the receptors' half-lives *in vivo* are unknown, it is still unclear what TGF-β type I receptors are present in or nearby the notochord during SB-505124 treatment. Therefore, it may be useful to generate transgenic lines possessing a tagged version of the receptor in question. Gene editing techniques, such as CRISPR-Cas9, could be used to add a small epitope tag, such as HA or FLAG, to the endogenous wild-type receptor. Though live imaging would not be possible and there would be concerns about the tag affecting receptor function, if the receptor functions normally then the presence of the receptor could be assayed through antibody stains of embryos fixed at any chosen developmental stage. We believe that tagging the carboxy terminus would be unlikely to significantly alter the receptor function because expression of a human ALK with an HA tag on the carboxy terminus was shown to successfully rescue TGF-β signaling in cell culture that was deficient in the ALK [10].

If the epitope tagged receptor lines successfully identify which TGF-β type I receptors are present in the notochord or nearby tissues, these lines could be used to test knockouts of the receptors. The simplest way to do so would be to use splice-blocking morpholinos. Since these morpholinos block splicing instead of translation, they will not affect early receptor expression from maternal mRNA, but only zygotically transcribed mRNA, so they will hopefully avoid any

early embryonic lethal phenotypes that would have resulted from a complete knockdown. Due to concerns about off-target effects of morpholinos though, a more complex and time-intensive method could use additional gene editing of the tagged line to add loxP sites flanking the gene of the receptor in question [22]. Homozygous floxed, epitope tagged fish would then be crossed with fish possessing Cre under control of a heatshock promoter. Using the *hsp*-Cre:LoxP-tagged receptor line, we would then heatshock embryos at various developmental timepoints and then use antibody staining to determine at what time heatshock results in a lack of the receptor in the notochord during the time of SB-505124 treatment. Following this determination, we would then grow up embryos that were heatshocked at the determined time to see if the abolishment of the receptor, or receptors, in notochord cells at the time of SB-505124 treatment is sufficient to induce tumorigenesis. If either of these approaches are sufficient to induce tumorigenesis, they would strongly suggest that SB-505124-induced tumor formation is due to its action on TGF-β type I receptors instead of any additional, novel effects, whereas a lack of tumorigenesis would leave open the possibility that SB-505124 possesses and additional, novel activity.

Using SB-505124-Induced Tumors for Drug Discovery

The rapamycin cotreatments strongly suggest that mTOR activity plays an important driving role in tumorigenesis, though the method by which SB-505124 treatment leads to mTOR activity is also unclear. The ability of rapamycin to decrease tumor incidence also means that rapamycin can be used as a positive control in future drug screening assays. Though our current measurements for tumors are a binary "is there a tumor or not?", the creation of *shha* ArB* and *shha* ArC lines driving fluorescence in early notochord and the tumors will allow the development of methods to estimate the size of the tumors. These methods will then be able to be

used in drug screens using the transgenic embryos to determine quantitatively if a drug slows or reverses the growth of SB-505124-induced tumors.

Comparison with Other Zebrafish Chordoma Models

Though we report a new chordoma model in zebrafish, there are two chordoma models in zebrafish that are already reported, so it is important to consider how accurately each model represents chordoma and whether the model can be used effectively in drug screening. Both previously reported models used H&E staining on tumor sections to compare cell morphology to that of chordomas. Their results both found tumors cells that were morphologically distinct from notochord cells, whereas the results of H&E staining on SB-505124-induced tumors found that the tumor cells closely resemble notochord cells that have overproliferated and migrated abnormally [13, 14]. Due to the morphological similarities, the other chordoma models were only tested for very few genetic markers of chordoma outside of *ta* [13, 14]. Neither of the studies reporting other zebrafish chordoma models make any mention of the diagnostic markers or of a transcriptome analysis for comparison with chordoma transcriptome data. Because of this, while we identified that chondrogenesis is likely playing a role in SB-505124-induced tumors, neither of the other models identify chondrogenesis in their tumors. Though this does not mean that chondrogenesis isn't going on in the other models, it leaves the possibility open that the mechanism leading to their chordoma-like phenotype may be substantially different compared to the actual mechanism by which chordomas form. This question is further asked of the HRASV12 driven model because HRAS mutations have not been reported in chordoma, whereas TGF-β signaling and PRL-3 have both been associated with chordomas [8, 13, 14]. Despite this, the HRASV12 driven tumors, like the SB-505124-induced tumors, are easy to form in large numbers, which makes them attractive models for drug screens [13]. The tumors driven by PRL-

3 overexpression are less suited to drug screens in their current state though, because they currently require that each embryo be injected with the mRNA [14]. Another similarity between the SB-505124-induced tumors and the HRASV12 driven tumors is their responsiveness to rapamycin, which was not tested in the PRL-3 overexpression tumors [13, 14]. The HRASV12 driven tumors were followed over time after rapamycin treatment, and it was found that the rapamycin treatment delayed, but did not abrogate, the tumor phenotype [13]. Though our rapamycin treatments decreased the tumor load and penetrance, we only counted the tumors at one time point, so it is possible that rapamycin treatment merely delayed the formation of SB-505124-induced tumors. The results of counting the tumors from these treatments multiple times over a period of days following treatment would allow us to compare more directly the SB-505124-induced tumors' response to rapamycin with that of the HRASV12 driven tumors.

Future Directions for a Zebrafish Chordoma Model

Though cotreatment with rapamycin decreased tumorigenesis in SB-505124 treated embryos, this only establishes that inhibition of mTOR activity acts in a prophylactic manner to decrease tumorigenesis. To see if inhibition of mTOR activity by rapamycin has any therapeutic properties on tumors that have already formed, embryos treated for 48 hours with a high penetrance SB-505124 concentration should be separated into those with evident tumors and those without. Those with evident tumors will have their current tumor count taken, and then will be treated with rapamycin or DMSO (vehicle). Following the second treatment, tumor counts should be taken again. This study will have the flaw though that there will only be an observable difference if a tumor is entirely abolished or the rate of additional tumor formation is decreased. To observe differences in individual tumors that may not be abolished, it will be necessary to

measure tumor size. Using one the *shha* ArB* or *shha* ArC lines, we first will need to develop a method of determining tumor size, which will likely be based off the largest circumference at a specified magnification because the tumors are roughly spherical. Using this measurement system, we can measure the size of tumors on an isolated embryo prior to and after the second treatment to determine if treatment with rapamycin slowed or reversed the growth of the tumor compared to that of DMSO treated embryos. In addition to its use with rapamycin studies, the method of measuring tumor size will be invaluable for screening drugs with therapeutic properties against the SB-505124-induced tumors. Large scale drug screens using the SB-505124-induced tumors though first requires solid proof of the tumors' ability to be a model for chordoma.

Though the initial RNAseq analysis dataset has promising accuracy and suggests more similarity of the SB-505124-induced tumors to chordomas than we had previously determined, it is not an optimal dataset to use because of the over-prevalence of short reads. With the improved fragmentation protocol, which should yield more average length reads, we hope to get a more complete RNAseq analysis dataset. The new RNAseq analysis dataset will then be verified using RNA *in situ* hybridizations to make sure that the transcripts that the dataset reports as being common in SB-505124-induced tumors are present in the tumors. Following successful verification, the new RNAseq analysis dataset can be compared with published chordoma RNAseq analysis datasets to identify similarities and differences in their top gene ontology terms. Ultimately, this comparison will help to determine whether our zebrafish model will be useful for drug discovery, with a reasonably good probability that a particular drug that works in the zebrafish model will also work in patients afflicted with chordomas.

References

1. Nibu Y, Jose-Edwards DS, Di Gregorio A: **From notochord formation to hereditary chordoma: the many roles of Brachyury**. *Biomed Res Int* 2013, **2013**:826435.
2. Yang XR, Ng D, Alcorta DA, Liebsch NJ, Sheridan E, Li S, Goldstein AM, Parry DM, Kelley MJ: **T (brachyury) gene duplication confers major susceptibility to familial chordoma**. *Nat Genet* 2009, **41**(11):1176-1178.
3. Cates JM, Itani DM, Coffin CM, Harfe BD: **The sonic hedgehog pathway in chordoid tumours**. *Histopathology* 2010, **56**(7):978-979.
4. Presneau N, Shalaby A, Idowu B, Gikas P, Cannon SR, Gout I, Diss T, Tirabosco R, Flanagan AM: **Potential therapeutic targets for chordoma: PI3K/AKT/TSC1/TSC2/mTOR pathway**. *Br J Cancer* 2009, **100**(9):1406-1414.
5. Derynck R, Zhang YE: **Smad-dependent and Smad-independent pathways in TGF-beta family signalling**. *Nature* 2003, **425**(6958):577-584.
6. Lamouille S, Derynck R: **Cell size and invasion in TGF-beta-induced epithelial to mesenchymal transition is regulated by activation of the mTOR pathway**. *J Cell Biol* 2007, **178**(3):437-451.
7. Cargnello M, Tcherkezian J, Roux PP: **The expanding role of mTOR in cancer cell growth and proliferation**. *Mutagenesis* 2015, **30**(2):169-176.
8. Wu Z, Wang L, Guo Z, Wang K, Zhang Y, Tian K, Zhang J, Sun W, Yu C: **Experimental study on differences in clivus chordoma bone invasion: an iTRAQ-based quantitative proteomic analysis**. *PLoS One* 2015, **10**(3):e0119523.
9. Agathon A, Thisse C, Thisse B: **The molecular nature of the zebrafish tail organizer**. *Nature* 2003, **424**(6947):448-452.
10. Wrana JL, Attisano L, Wieser R, Ventura F, Massague J: **Mechanism of activation of the TGF-beta receptor**. *Nature* 1994, **370**(6488):341-347.
11. Stoletov K, Klemke R: **Catch of the day: zebrafish as a human cancer model**. *Oncogene* 2008, **27**(33):4509-4520.
12. Terriente J, Pujades C: **Use of zebrafish embryos for small molecule screening related to cancer**. *Dev Dyn* 2013, **242**(2):97-107.
13. Burger A, Vasilyev A, Tomar R, Selig MK, Nielsen GP, Peterson RT, Drummond IA, Haber DA: **A zebrafish model of chordoma initiated by notochord-driven expression of HRASV12**. *Dis Model Mech* 2014, **7**(7):907-913.
14. Li L, Shi H, Zhang M, Guo X, Tong F, Zhang W, Zhou J, Wang H, Yang S: **Upregulation of metastasis-associated PRL-3 initiates chordoma in zebrafish**. *Int J Oncol* 2016, **48**(4):1541-1552.
15. DaCosta Byfield S, Major C, Laping NJ, Roberts AB: **SB-505124 is a selective inhibitor of transforming growth factor-beta type I receptors ALK4, ALK5, and ALK7**. *Mol Pharmacol* 2004, **65**(3):744-752.
16. Hagos EG, Dougan ST: **Time-dependent patterning of the mesoderm and endoderm by Nodal signals in zebrafish**. *BMC Dev Biol* 2007, **7**:22.
17. Harvey SA, Tumpel S, Dubrulle J, Schier AF, Smith JC: **no tail integrates two modes of mesoderm induction**. *Development* 2010, **137**(7):1127-1135.
18. Muller F, Chang B, Albert S, Fischer N, Tora L, Strahle U: **Intronic enhancers control expression of zebrafish sonic hedgehog in floor plate and notochord**. *Development* 1999, **126**(10):2103-2116.

19. Fleming A, Keynes R, Tannahill D: **A central role for the notochord in vertebral patterning**. *Development* 2004, **131**(4):873-880.
20. Stacchiotti S, Marrari A, Tamborini E, Palassini E, Virdis E, Messina A, Crippa F, Morosi C, Gronchi A, Pilotti S *et al*: **Response to imatinib plus sirolimus in advanced chordoma**. *Ann Oncol* 2009, **20**(11):1886-1894.
21. Amores A, Force A, Yan YL, Joly L, Amemiya C, Fritz A, Ho RK, Langeland J, Prince V, Wang YL *et al*: **Zebrafish hox clusters and vertebrate genome evolution**. *Science* 1998, **282**(5394):1711-1714.
22. Kok FO, Shin M, Ni CW, Gupta A, Grosse AS, van Impel A, Kirchmaier BC, Peterson-Maduro J, Kourkoulis G, Male I *et al*: **Reverse genetic screening reveals poor correlation between morpholino-induced and mutant phenotypes in zebrafish**. *Dev Cell* 2015, **32**(1):97-108.

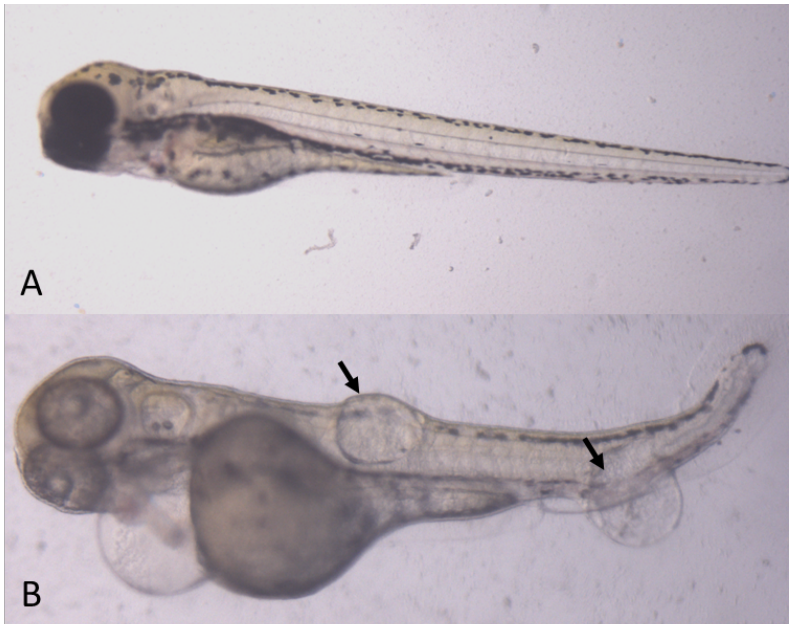

Figure 1: SB-505124 induces tumor formation. Light microscopy of living WT embryos (5 dpf) treated with vehicle (A) or 40µM SB-505124 (B). Tumors indicated by arrows.

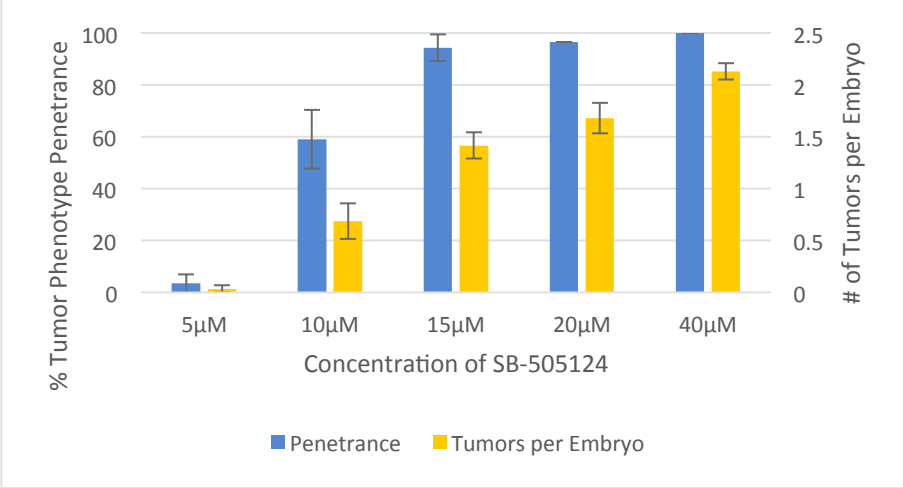

Figure 2: Tumor phenotype penetrance is correlated with SB-505124 concentration. Relationship between SB-505124 concentration and the penetrance of the tumor phenotype or the number of tumors per embryo. Error bars are +/- one standard deviation. n=3 dishes of ~30 embryos in each situation.

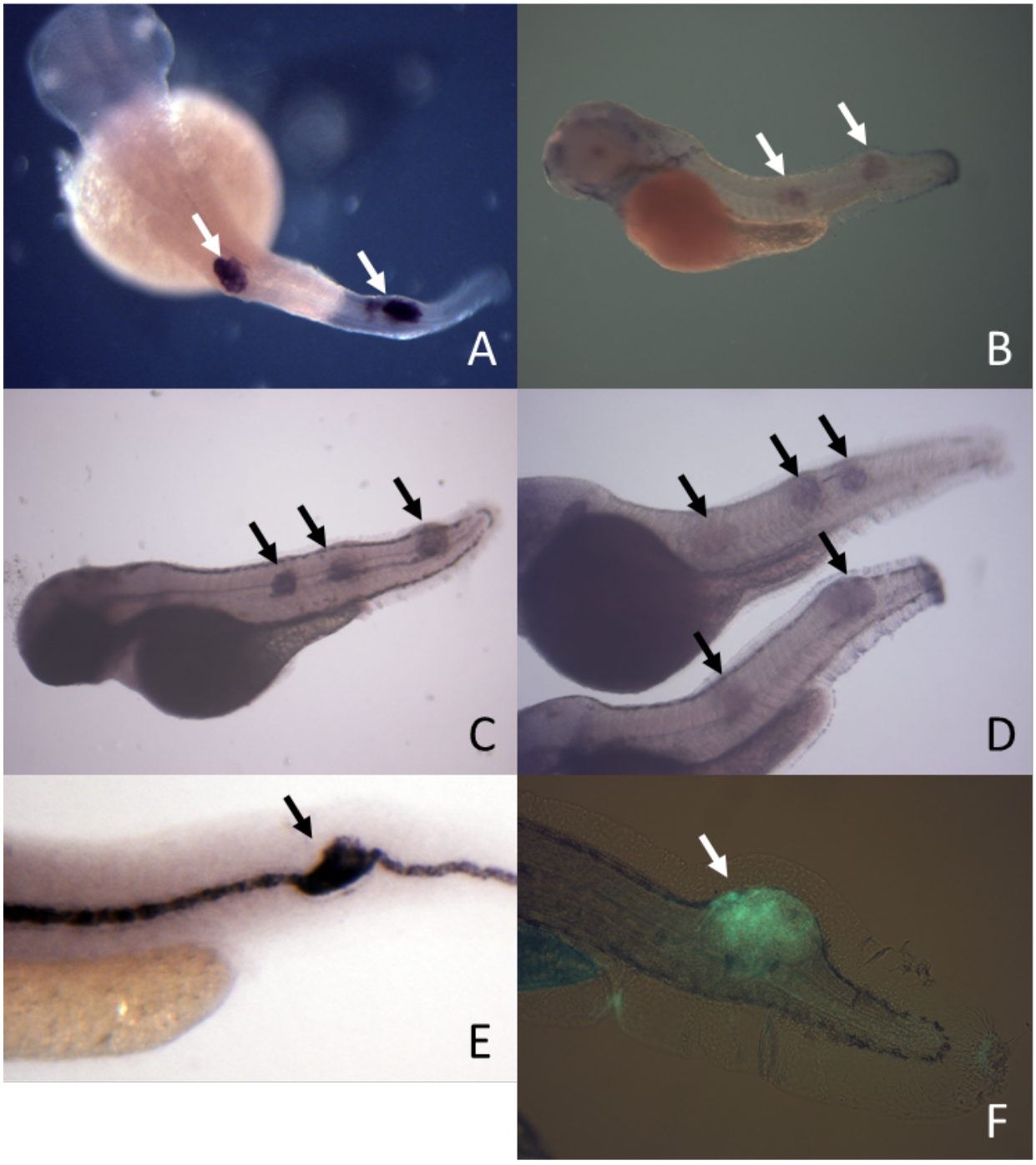

Figure 3: Initial characterization of 3-4dpf SB-505124 treated embryos. A-E are RNA *in situ* hybridizations for *ta* (A), *tb* (B), *shha* (C), *shhb* (D), and *col2a1a* (E). F is an antibody stain against pS6. Tumors indicated by arrows.

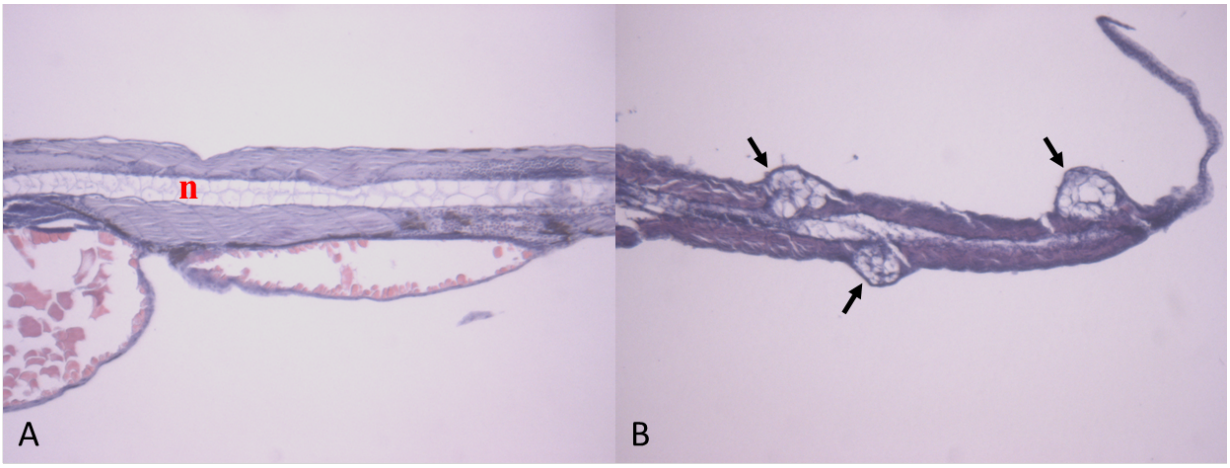

Figure 4: Histology of control notochord and tumors. H&E staining of 5dpf DMSO (A) or SB-505124 (B) treated embryos. Notochord of DMSO treated embryos indicated by **n**, tumors indicated by arrows.

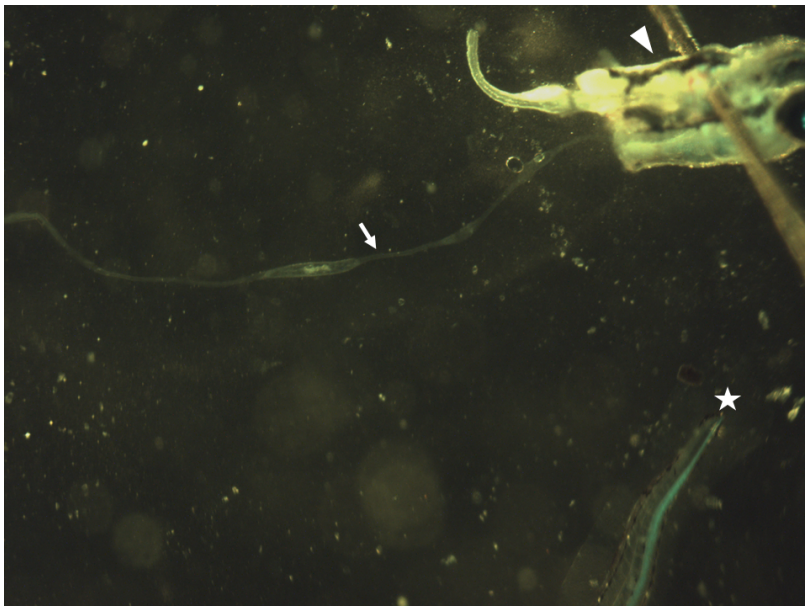

Figure 5: Notochord dissection. Mid-dissection of fluorescent notochords. Arrow indicates dissected out notochord portion still connected to a trunk segment (indicated by arrowhead). Star indicates the tail end of an undissected notochord inside a second embryo.

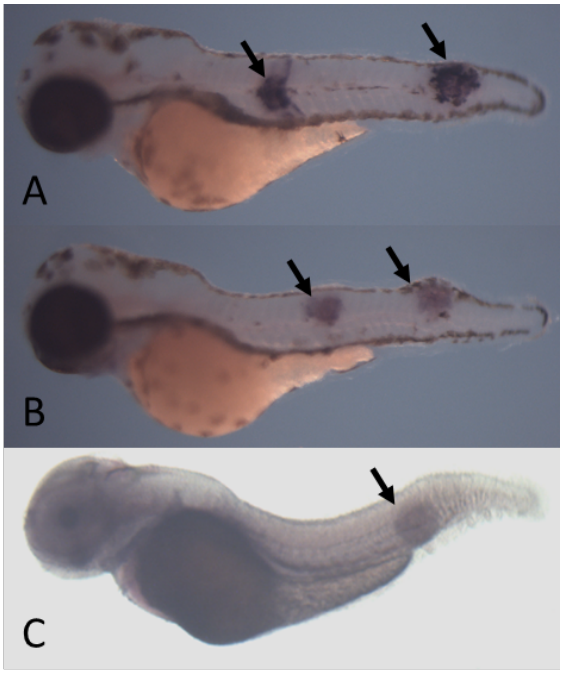

Figure 6: SB-505124-induced tumors express *ngs*, *ehd2b*, and *c7a*. RNA *in situ* hybridizations of SB-505124-induced tumor markers identified during attempting microarray validation on 4-5dpf SB-505124 treated embryos. Probes: *ngs* (A), *ehd2b* (B), and *c7a* (C).

gene_assignment	Gene Symbol	RefSeq	p-value	Ratio(Exp vs. Ctrl)	Fold-Change(Exp vs. Ctrl)
BC162297 // ntla // no tail a // --- // 30399 /// BC162300 // ntla // no tail a // ---	ntla	BC162297	0.23617	0.699618	-1.42935
XM_001343597 // LOC100004296 // novel protein similar to murine T brachyury (T) // ---	LOC100004296	XM_001343597	0.01188	0.135044	-7.40501
L27585 // shha // sonic hedgehog a // --- // 30269 /// U30711 // shha // sonic hedgehog	shha	L27585	0.11301	0.49719	-2.0113
U30710 // shhb // sonic hedgehog b // --- // 30444 /// BC078321 // shhb // sonic hedgeh	shhb	U30710	0.06981	0.0532109	-18.7932

Figure 7: Microarray entries of known SB-505124-induced tumor markers. The microarray entries for *ta* (formerly known as *ntla*), *tb* (LOC100004296, at the time unnamed), *shha*, and *shhb*.

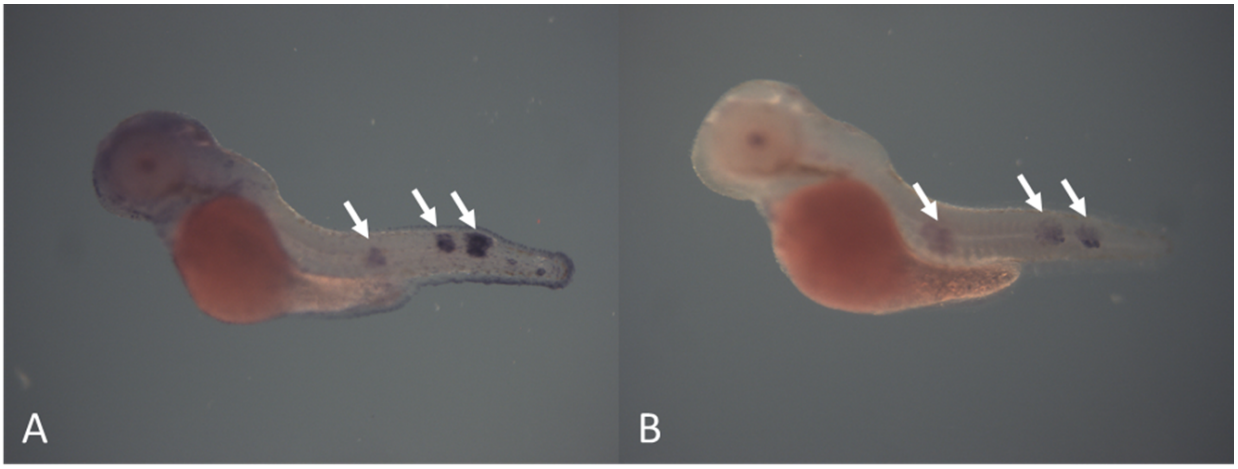

Figure 8: SB-505124-induced tumors express *ptrfb* and *sncga*. RNA *in situ* hybridizations of genes selected from the initial RNAseq dataset on 3-4dpf SB-505124 treated embryos. Probes: *ptrfb* (A) and *sncga* (B).

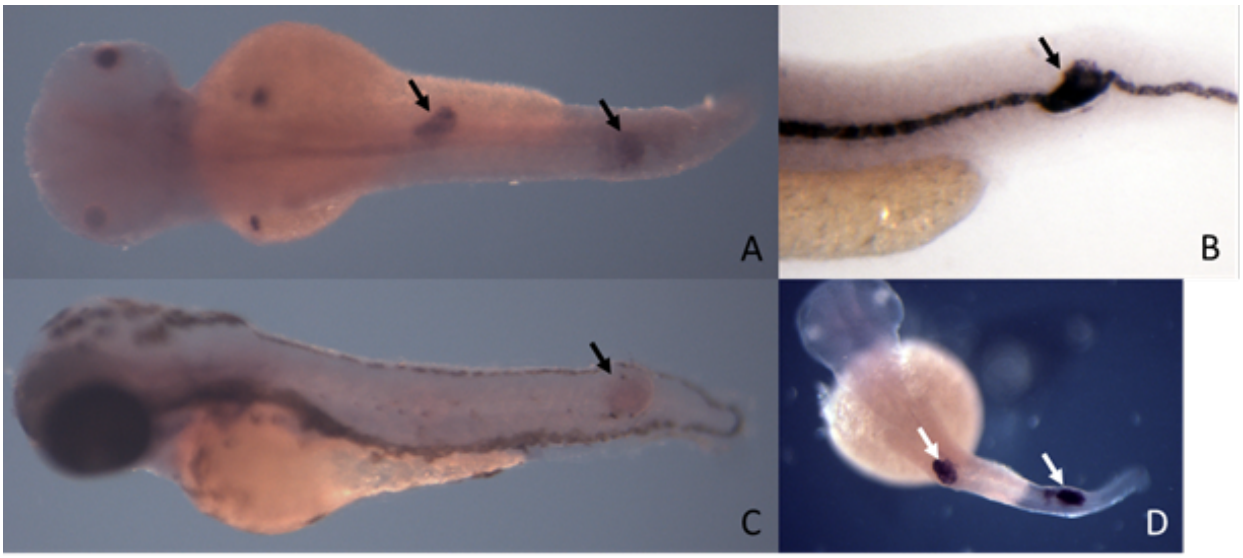

Figure 9: SB-505124-induced tumors express 4 chordoma diagnostic marker genes. RNA *in situ* hybridizations of chordoma diagnostic marker genes that were expressed in tumors on 3-4dpf SB-505124 treated embryos. Probes: *acanb* (A), *col2a1a* (B), *cspg4* (C), and *ta* (D).

	tgfbr1a	tgfbr1b	acvr1ba	acvr1bb	acvr1c	acvr1
bud	nc+	nc+	nc+	nc+	N/A	N/A
2s	nc+	nc+	nc+	nc+	N/A	nc+
5s	N/A	N/A	nc+	nc+	N/A	N/A
8-10s	AS	N/A	AS	AS	N/A	N/A
10s	N/A	somites, AS	not nc	not nc	not nc	not nc
12-14s	not nc	somites, AS	not nc	not nc	not nc	not nc
14-16s	not nc	somites, AS	N/A	N/A	N/A	not nc
20-21h	N/A	N/A	N/A	N/A	not nc	N/A
24h	not nc	N/A	N/A	N/A	N/A	N/A
30h	not nc	N/A	N/A	N/A	N/A	N/A

Table 1: Expression of ALK4, ALK5, and ALK7 orthologs in zebrafish. Summarized results of RNA *in situ* hybridizations for ALK4, ALK5, and ALK7 orthologs in zebrafish. Columns are genes, rows are the developmental stage tested. N/A were combinations not tested. AS represents an unidentified axial structure. The RNA *in situ* hybridizations are available in **Appendix: TGF-β Receptor *in situ* Hybridizations**.

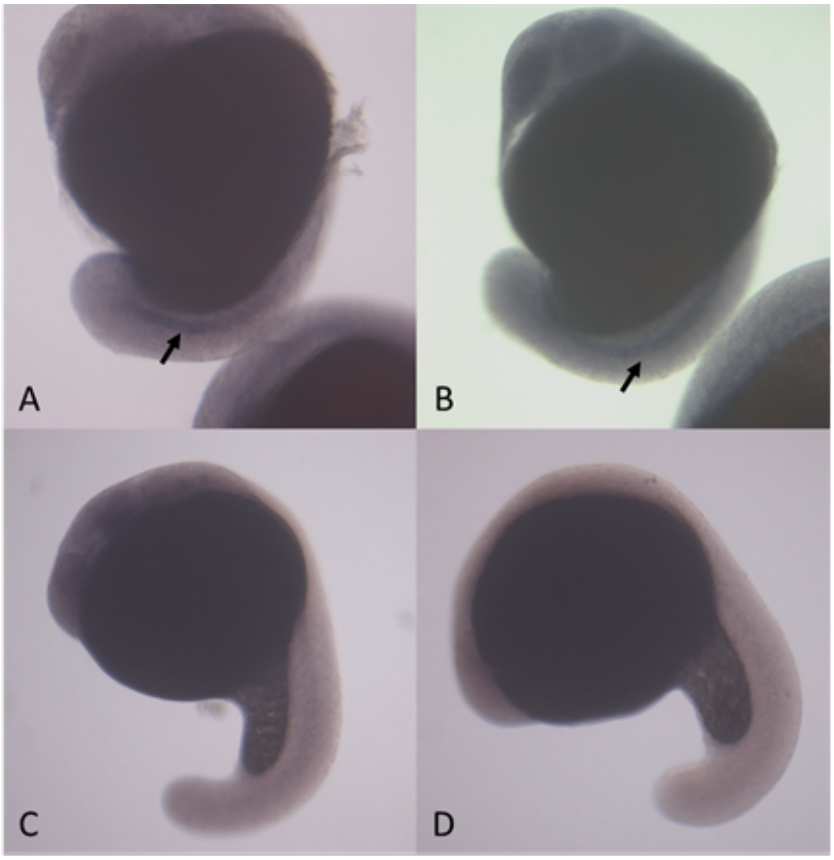

Figure 10: Expression patterns of TGF-β and Activin ligands. RNA *in situ* hybridizations for ligands of ALK4, ALK5, and ALK7 receptors on SB-505124 treated embryos. Probes and stage: *tgfb2* (16-somite) (A), *tgfb3* (16-somite) (B), *inhbb* (20-somite) (C), and *inhbab* (20-somite) (D).

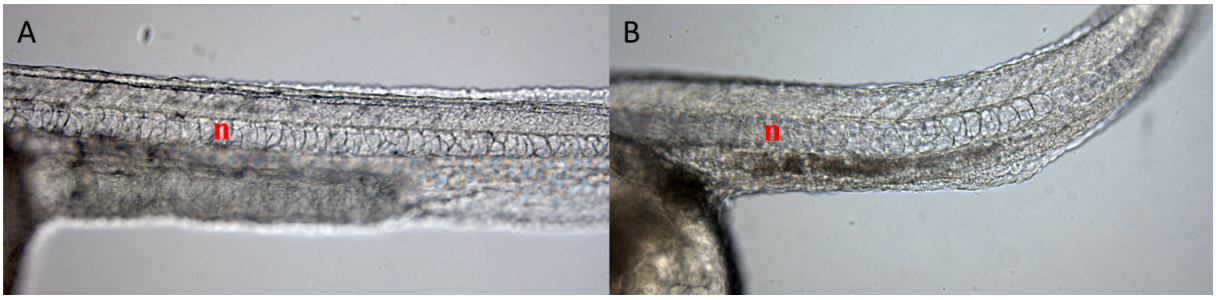

Figure 11: Morpholino-induced knockdown of *tgfb2*/*tgfb3* does not cause notochord tumors. Light microscopy of ~28 hours post-fertilization WT (A) and *tgfb2*/*tgfb3* knockdown morphant (B) embryos. **n** labels the notochord.

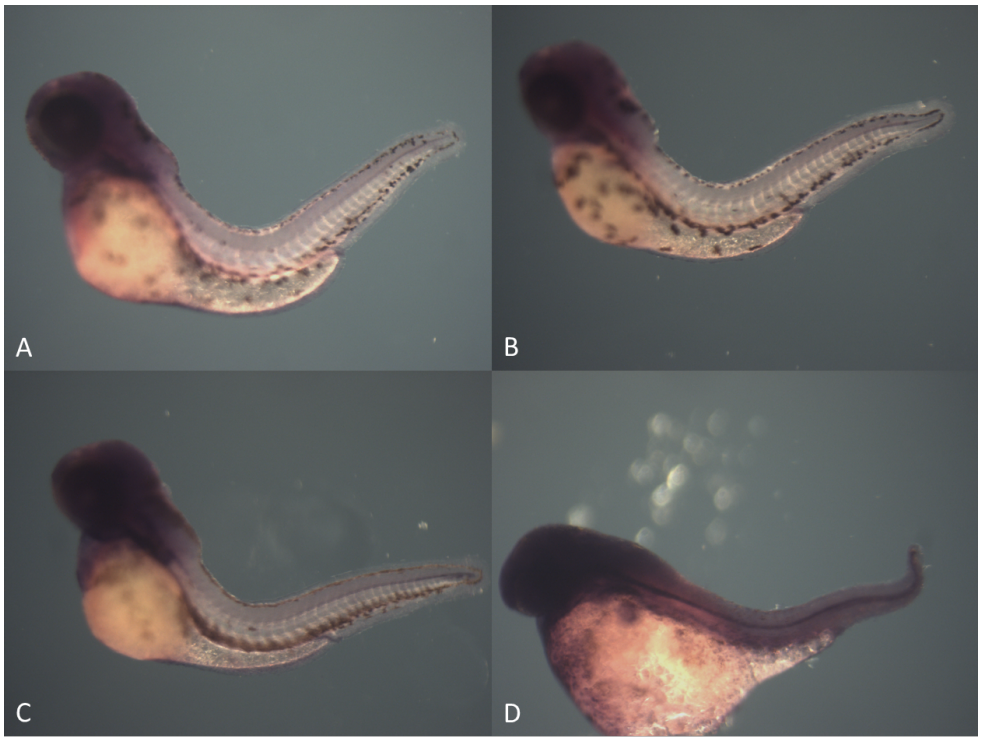

Figure 12: Alternative inhibitors of ALK4, ALK5, and ALK7 do not cause notochord tumors. RNA *in situ* hybridization for *shha* in 3dpf embryos following treatment with alternative ALK4, ALK5, and ALK7 inhibitors. SB-431542 and GW788388 are at maximal doses, A83-01 and SD-208 are at submaximal doses in order to achieve a more moderate phenotype. SB-431542 at 600µM (A), GW788388 at 200µM (B), A83-01 at 20µM (C), and SD-208 at 10µM (D).

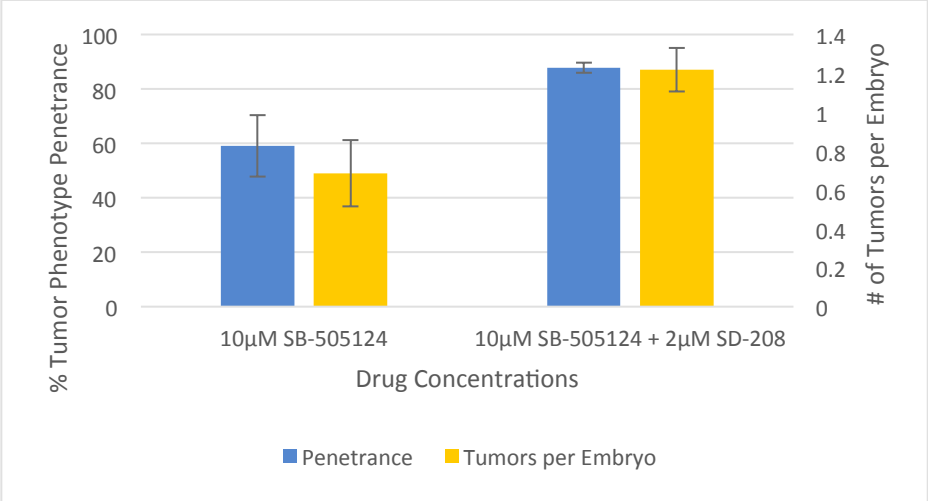

Figure 13: Cotreatment with SD-208 increases the penetrance of the SB-505124-induced tumor phenotype. The effect of 2µM SD-208 cotreatment on the tumor phenotype penetrance and number of tumors per embryo of 10µM SB-505124. Error bars are +/- one standard deviation. n=3 dishes of ~30 embryos in each situation.

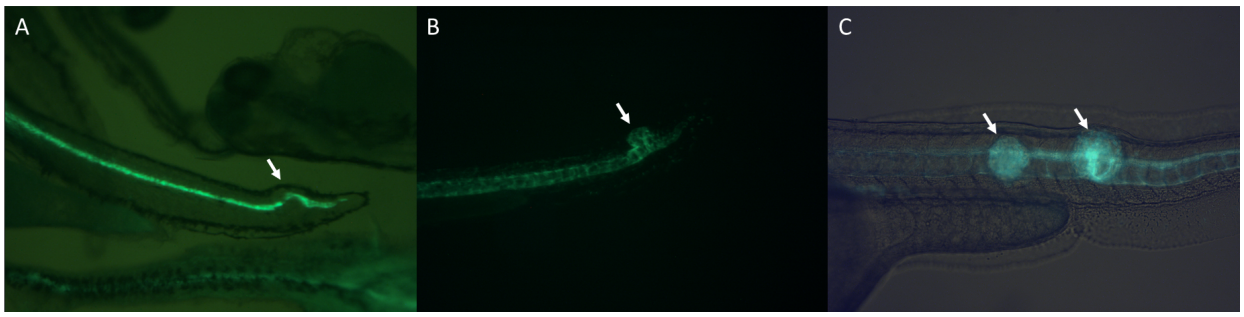

Figure 14: Transgenic lines expressing fluorescent protein in notochord and tumor cells. Fluorescence microscopy of 2dpf (A, B) or 4dpf (C) SB-505124 treated *shha* ArB (A), *shha* ArB* (B), and *shha* ArC (C) embryos. *Shha* ArB expresses GFP in the floorplate, *shha* ArB* and *shha* ArC express GFP and Kaede, respectively, in the notochord and tumors.

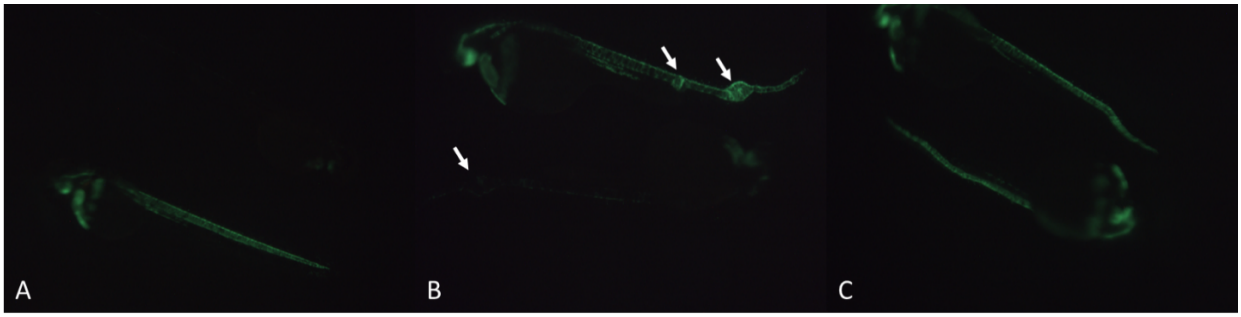

Figure 15: Decreased tumor formation in rapamycin cotreatment. Fluorescence microscopy of ~2dpf DMSO (A), 40µM SB-505124 (B), or 40µM SB-505124 and 10µM rapamycin (C) treated *shha* ArC embryos. In figures B and C, the embryo on top is positioned with the anterior to the left and the embryo on bottom is positioned with the anterior to the right and upside down.

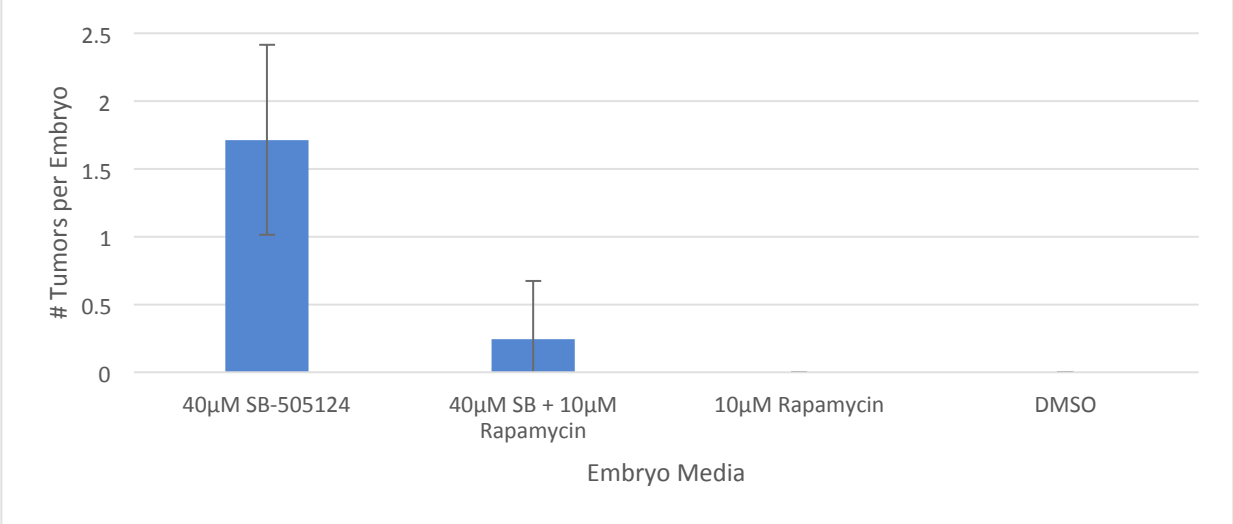

Figure 16: Rapamycin cotreatment significantly decreases the tumor prevalence in SB-505124 treated embryos. Quantification of tumorigenesis in 5dpf embryos treated with 40µM SB-505124 or 40µM SB-505124 and 10µM Rapamycin. Error bars are +/- one standard deviation. n=70, 78, 88, and 88. P<0.0001. P value calculated using a two-tailed unpaired t test.

Appendix: TGF-β Receptor *in situ* Hybridizations

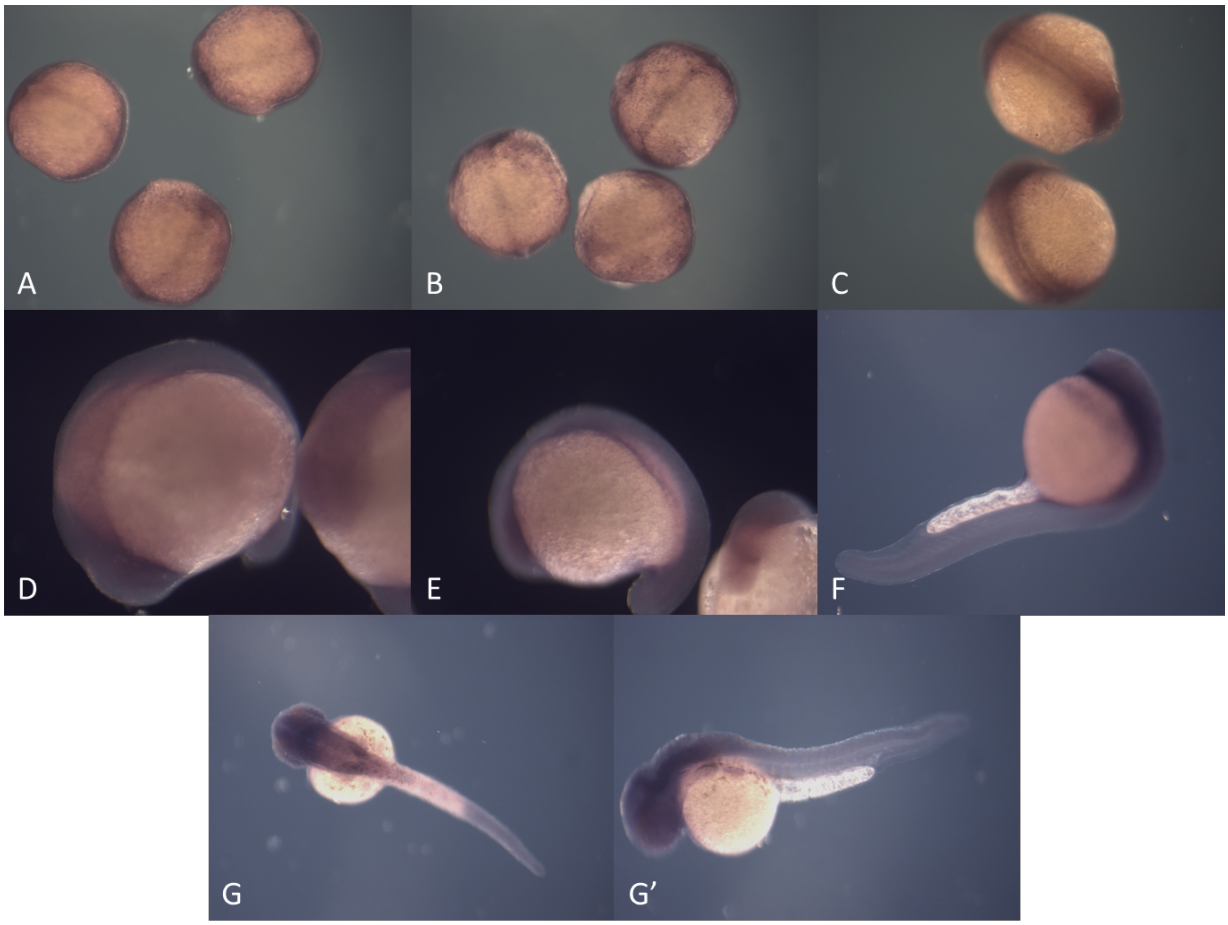

Figure A1: Expression of *tgfbr1a* in wild-type embryos. *tgfbr1a* bud (A), 2s (B), 8-10s (C), 12-14s (D), 14-16s (E), 24h (F), 30h dorsal (G), 30h lateral (G')

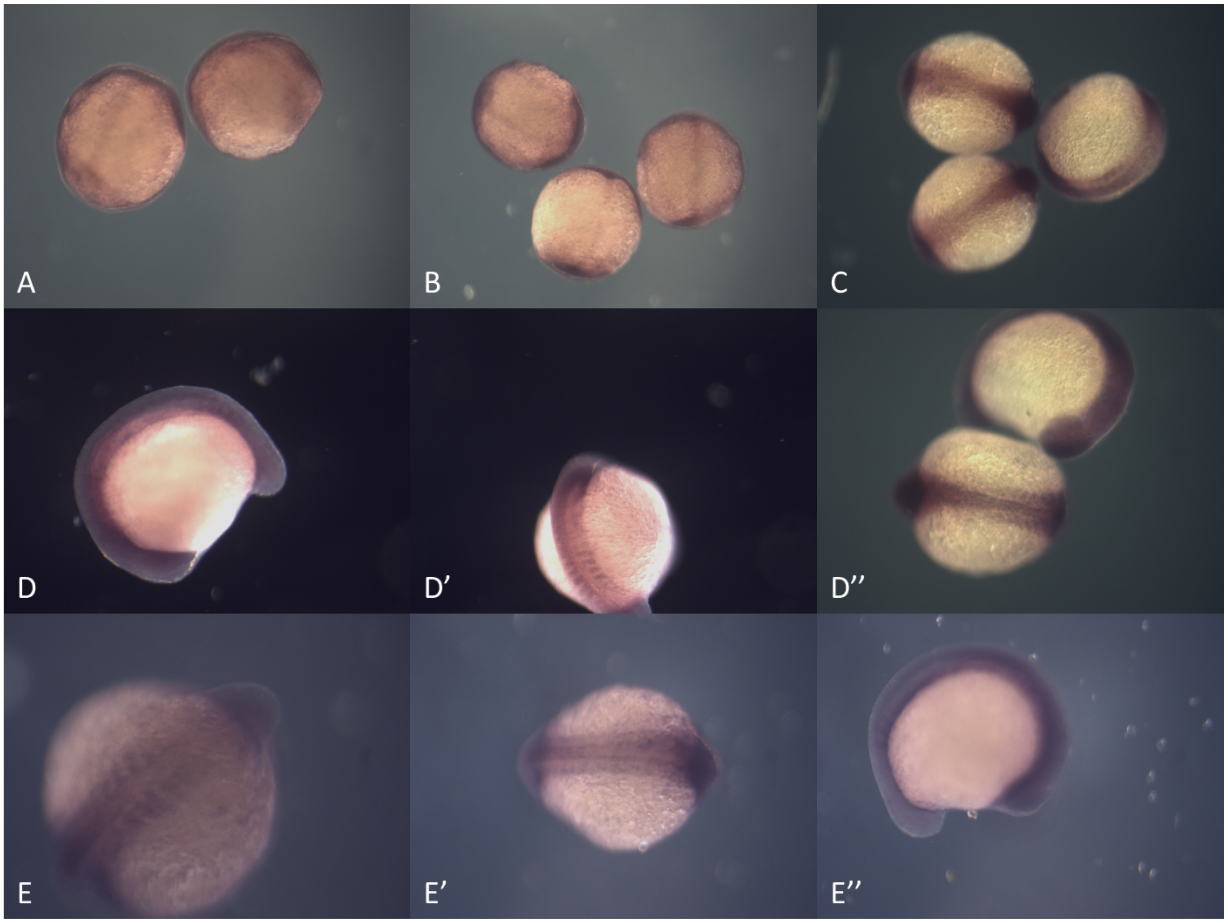

Figure A2: Expression of *tgfbr1b* in wild-type embryos. *tgfbr1b* bud (A), 2s (B), 10s (C), 12-14s (D), 14-16(E, E', E'')

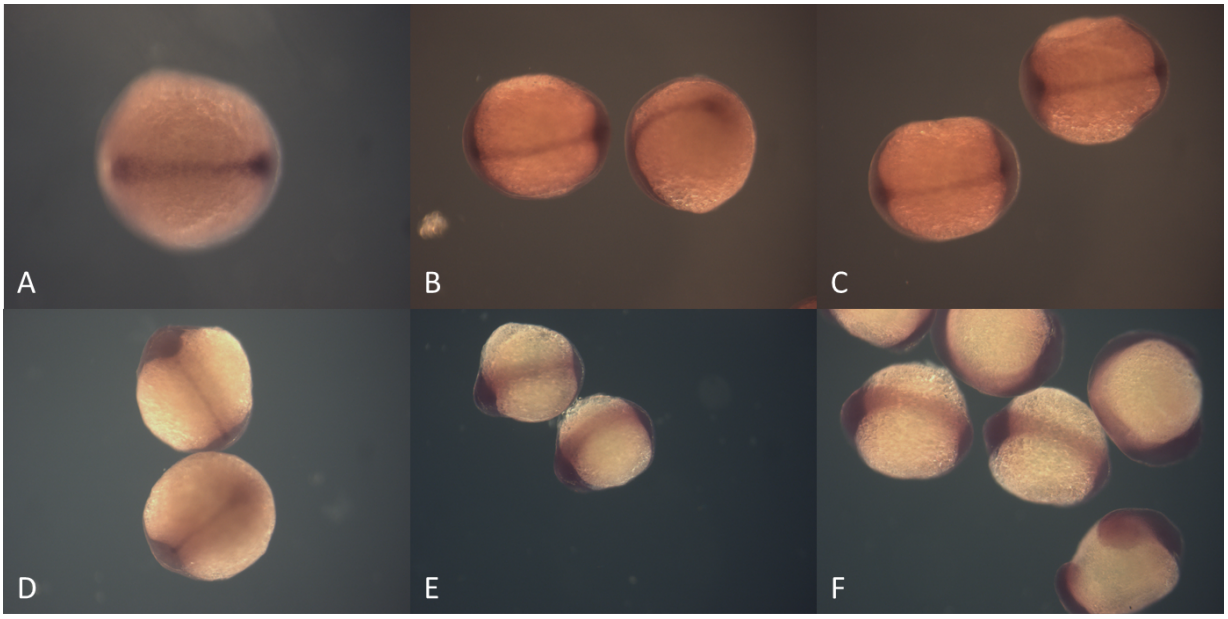

Figure A3: Expression of *acvr1ba* in wild-type embryos. *acvr1ba* bud (A), 2s (B), 5s (C), 8-10s (D), 10s (E), 12-14s (F)

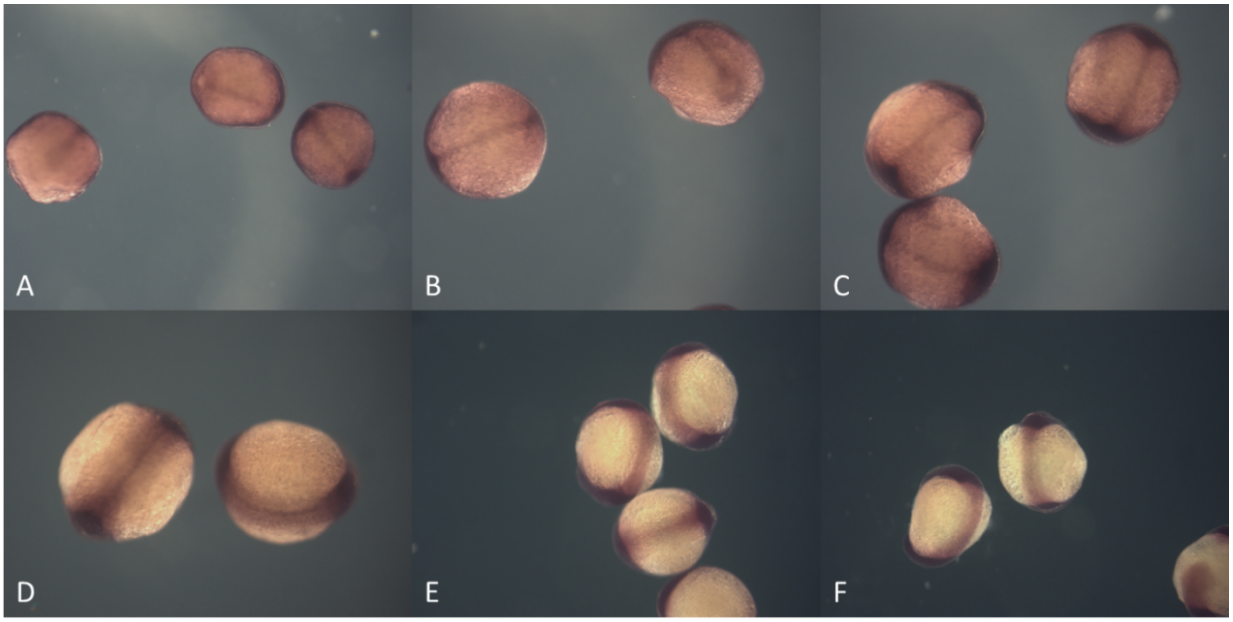

Figure A4: Expression of *acvr1bb* in wild-type embryos. *acvr1bb* bud (A), 2s (B), 5s (C), 8-10s (D), 10s (E), 12-14s (F)

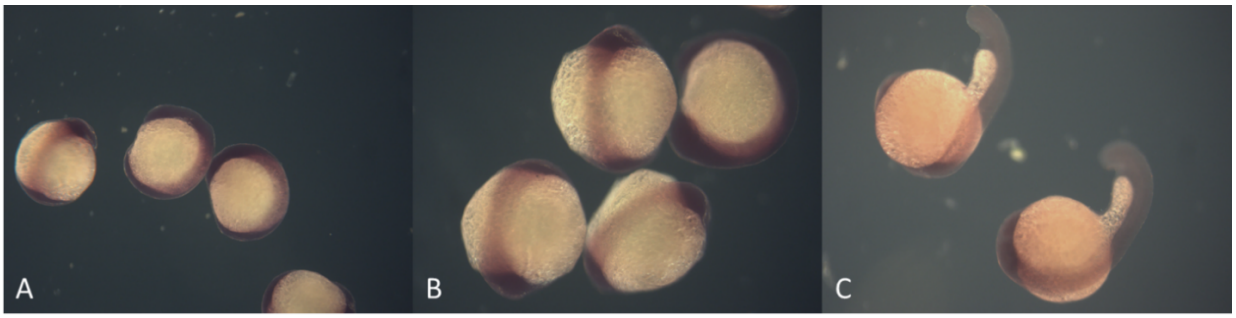

Figure A5: Expression of *acvr1c* in wild-type embryos. *acvr1c* 10s (A), 12-14s (B), 20-21h (C)

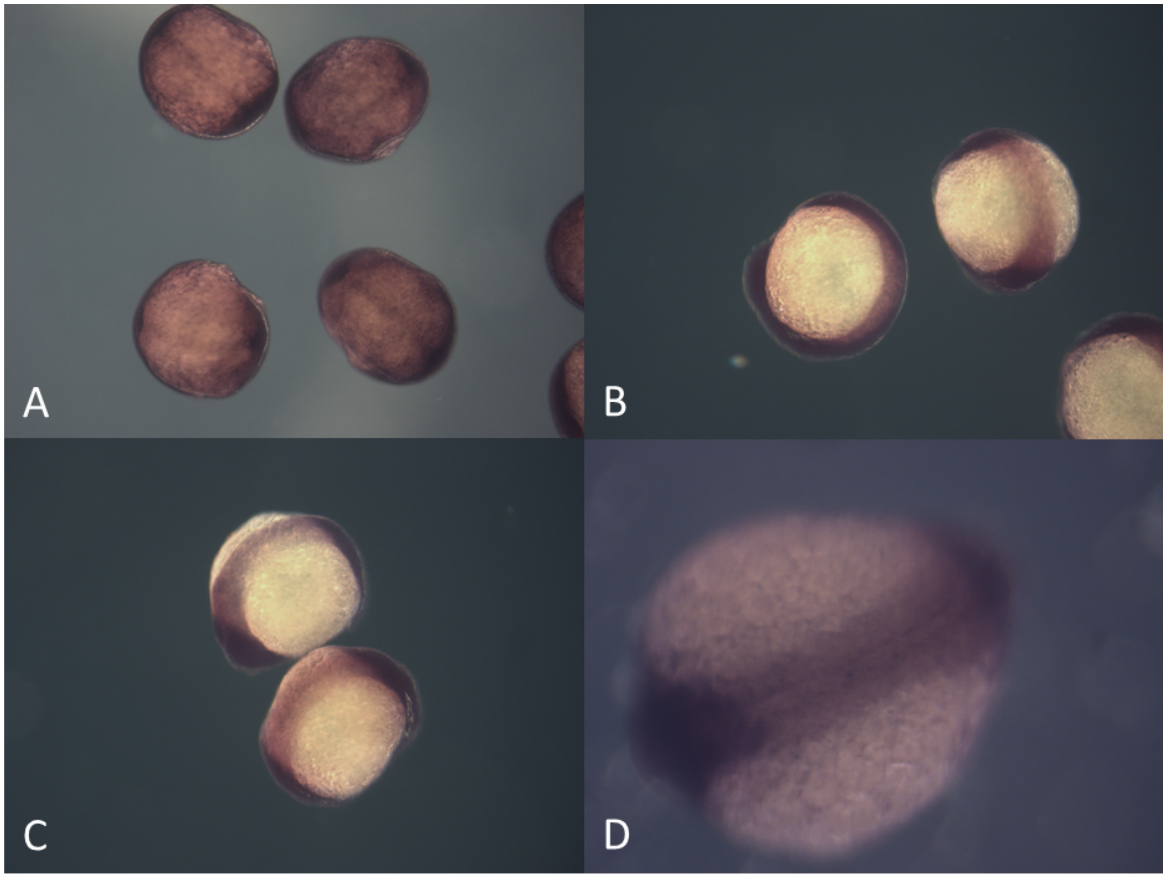

Figure A6: Expression of *acvr1* in wild-type embryos. *acvr1* 2s (A), 10s (B), 12-14s (C), 14-16s (D)